Advanced Methods for Atmospheric Modeling

by

Laura C. Rodman

NEAR TR 420
January 1991

NEAR inc

Copy No. 3

REPORT DOCUMENTATION PAGE

Form Approved
OMB No. 0704-0188

1. AGENCY USE ONLY (Leave blank)	2. REPORT DATE	3. REPORT TYPE AND DATES COVERED
	31 JAN 91	Final Technical, 1 JUL 90 - 31 DEC 90

4. TITLE AND SUBTITLE

Advanced Methods for Atmospheric Modeling

5. FUNDING NUMBERS

F49620-90-C-0040

61102F 3005/A1

6. AUTHOR(S)

Rodman, Laura C.

7. PERFORMING ORGANIZATION NAME(S) AND ADDRESS(ES)

Nielsen Engineering & Research, Inc.
510 Clyde Avenue
Mountain View, CA 94043-2287

8. PERFORMING ORGANIZATION REPORT NUMBER

NEAR TR 420

9. SPONSORING/MONITORING AGENCY NAME(S) AND ADDRESS(ES)

Air Force Office of Scientific Research
Building 410
Bolling AFB, DC 20332-6448

NC

10. SPONSORING/MONITORING AGENCY REPORT NUMBER

11. SUPPLEMENTARY NOTES

12a. DISTRIBUTION/AVAILABILITY STATEMENT

distribution unlimited; approved for public release

12b. DISTRIBUTION CODE

A

13. ABSTRACT *(Maximum 200 words)*

The evolution of physical processes in a numerical simulation of the atmosphere and the effects of their interactions on a forecast are very complex and difficult to isolate. An analysis was developed which uses artificial intelligence techniques to study the time-evolving quantities in a numerical simulation in order to determine the relationships among various flow parameters. This procedure was divided into two parts. First, the data was manipulated into a form that allowed the relationships of interest to be isolated. In particular, it was necessary to be able to see how several quantities may interact to affect the solution. The next step used an expert system to analyze the data based on these relationships. The test problem chosen was the numerical simulation of the decay of turbulence in a stratified fluid. Three different analyses were used to determine sensitivities, comparisons, and correlations among the flow quantities. The automation of this technique allowed the processing of the large amounts of data that were generated by a numerical simulation. For the test case, this method was able to draw similar conclusions about the nature of the flow solution compared with those given in the literature.

14. SUBJECT TERMS	15. NUMBER OF PAGES
atmospheric sciences, artificial intelligence	43
	16. PRICE CODE

17. SECURITY CLASSIFICATION OF REPORT	18. SECURITY CLASSIFICATION OF THIS PAGE	19. SECURITY CLASSIFICATION OF ABSTRACT	20. LIMITATION OF ABSTRACT
UNCLASSIFIED	UNCLASSIFIED	UNCLASSIFIED	UL

RESEARCH OBJECTIVES

The evolution of physical processes in the atmosphere and the effects of their interactions are very complex and difficult to isolate. These processes and interactions are typically studied with experimental or computational models that represent an aspect of atmospheric dynamics. However, even the model problems are quite complex and the underlying physics may be difficult to observe. Although numerical models of atmospheric flows can provide very detailed spatial and temporally evolving data, the sheer volume of this data makes it a difficult task to study all of the interactions within the solution.

Investigators who are studying the relationships among various flow quantities in a time-accurate simulation can "follow the action" if the number of flow quantities of interest is on the order of three or less. This corresponds to a solution space that is no more than three dimensions and can be easily represented in a graphical form. However, as the number of quantities involved in an interaction increases, the solution space has more than three dimensions, and the representation of the data becomes more complex and may hinder the understanding of the results.

The objective of this work is to investigate the feasibility of combining artificial intelligence methods with numerical flow simulations to use as a tool for studying the fundamental processes occurring in atmospheric flows. This work is based on the idea that an investigator can formulate a process for studying physical interactions involving a few variables, and that this process can be programmed onto a computer. Then, the computer can extrapolate the process to a higher dimensional problem, allowing it to distill the results to find the most useful information and present that information to the researcher in an easily understood form. The term "artificial intelligence" is used here to mean this technique of programming a computer to follow the same deductive processes that a person would use in performing a certain task. In the present case, the advantage to automating the task with a computer is that large amounts of data may be analyzed much more quickly than if the job were performed manually. The artificial intelligence program is used as a postprocessor to the numerical simulation which assists the investigator in the task of filtering the data.

A program that has been written for this purpose, CHASE (Characterization and Search), was initially developed to study how certain flow quantities are affected by the input variables. The output of this code was the determination of the numerical range of the input variables which most strongly affected the output quantities, as well as how all of the variables interacted to produce the strongest effect on the flow field.[1] This filtering of the results allowed the researcher to concentrate on the inputs that had the greatest effect on the solution and to disregard those inputs that had little or no effect.

In the present work, this code was extended and applied in a somewhat different manner. Instead of treating a problem exclusively as output vs. input, the program was also able to look at many time-varying flow quantities vs. each other. This allowed the code to characterize the relationships among several physical quantities in the solution, as well as their dependence on the problem input values. A major effort in this work was the extension to CHASE of the capability to study different aspects of a time-evolving solution.

Another effort was the identification of problems associated with this approach and suggested methods to solve these problems in future work.

STATUS OF RESEARCH EFFORT

Model Problem

The model problem chosen for this work was the numerical simulation of the decay of isotropic homogeneous turbulence in a stably stratified fluid. This problem has been studied experimentally and numerically and the results are well documented,[2-4] providing a comparison for the present work. The bouyancy in a stable fluid acts to limit the size of the vertical turbulent scales, so that initially isotropic turbulence decays to a combination of gravity waves and large scale horizontal motions. This problem was particularly well-suited to the characterization process as there are many time-dependent flow quantities that interact with each other. Previous researchers have looked in particular at the various length scales of the flow, the energetics, and the bouyancy flux.

Computational Model

A computational flow model for the test case has been developed. The Navier-Stokes code TMRC, developed at NEAR, was used. A large eddy simulation was performed on a 32x32x32 Cartesian grid. The algorithm used was a fourth-order accurate explicit finite volume method, and the Smagorinsky sub-grid scale turbulence model was employed.

The code TMRC was chosen because it had been written in-house, so the investigators working on this contract were familiar with it. However, as the code solves the compressible Navier-Stokes equations, certain direct comparisons with incompressible solutions cannot be made, particularly since the divergence-free velocity condition is not enforced with this code. In addition, all of the flow variables in TMRC, including the gravitational acceleration and the Brunt-Vaisala frequency, are normalized with the ambient sound speed. Thus, a direct comparison of the degree of stratification between this model and an incompressible model is difficult.

The initial conditions are generated in a manner similar to that described in References 4 and 5. The spectra of the initial velocity field is chosen to have amplitude $E(k) = Ck^4\exp(-2(k/k_m)^2)$, with the peak energy at $k_m = 4.760$.[4] The spectral amplitudes are used to find the magnitudes of the Fourier transform of the velocities. Statistical isotropy is then generated by randomly choosing the direction of the Fourier transformed velocity vectors at each point in wavespace.[5] These vectors are constrained to lie in the plane that is perpendicular to the wave vector, thus ensuring continuity. The inverse transform is used to generate the fluctuating velocity field. The flow solution from these initial conditions is run out for a short time to allow the statistics to acquire the behavior of a turbulent flow field, and the resulting solution is used as the initial conditions for subsequent calculations. This initial condition also has an associated fluctuating density and pressure field.

Stratification is imposed on the flow field in the following manner. First the turbulent length scales for the unstratified initial conditions are found. These quantities are used to

pick a Brunt-Vaisala frequency that will provide a particular microscale Froude number. As this frequency will be nondimensionalized with the sound speed in this work, it will not match the values reported by other investigators. Since the compressible equations are being solved in this work, the Brunt-Vaisala frequency is defined as

$$N^2 = \frac{g}{T}\left[\frac{\partial T}{\partial z} + \frac{g}{c_p}\right] \tag{1}$$

This equation allows the solution of T(z), given the value of N and g. The equation of state (with the gas constant R taken to be unity) is

$$p(z) = \rho(z)T(z) \tag{2}$$

and the vertical momentum equation (with zero mean velocity) is

$$\partial p/\partial z = -\rho g \tag{3}$$

Once N and g are specified, these equations allow the solution of the mean pressure and density as a function of vertical distance in the stratified field (see Appendix A). Although N can be chosen based on the desired Froude number, g is chosen to give reasonable values of the density, temperature, and pressure gradients over the computational domain. For instance, the density and pressure gradients must be small enough that the mean values of either density or pressure are larger than the fluctuating value at the top of the domain. Also, for computational efficiency, the temperature should not get large enough to greatly increase the local speed of sound, since the time step in TMRC varies inversely with the maximum local sound speed. It was found that values of (nondimensional) g approximately equal to the (nondimensional) N gave the most reasonable gradients. Figure 1 shows the values of the these variables plotted against height.

The boundary conditions used are periodic in all directions for the fluctuating quantities, and the mean density and pressure are modified in the vertical direction to account for the stratification. The computational domain extends from 0 to 2π in all three directions, which allows for integer wavenumbers from 0 to 16. The initial rms turbulence fluctuations are chosen to give a Mach number of 0.2. The mean flow has zero velocity. The Reynolds number based on unit length and the initial rms velocity is chosen to be 1000.

Input and Output Quantities

Flow quantities of interest are chosen that will characterize the solution, and these must be computed and saved at representative time steps. The relationships between these quantities are what will be determined by the characterization code. Flow quantities that have been identified as relevant in the literature are given in Table 1. A postprocessor to the Navier-Stokes code (preprocessor to CHASE) that computes these quantities and stores them at representative times has been written.

Computational Results

A series of computations has been run for three values of N. The first case is unstratified, with N and g both equal to zero. The second case is moderately stratified with N = 0.045 and g = 0.045, giving an initial turbulent Froude number of 4. The third case is more strongly stratified, with N = 0.0915 and g = 0.09, and an initial Froude number of 2.

Figure 2 shows density contours in a horizontal and vertical plane at the moderate stratification level, at a time that is approximately thirty percent of one Brunt-Vaisala period. Although there are many eddies present in the horizontal plane (Figure 2a), the density clearly indicates a wave pattern in the vertical plane (Figure 2b). In Figure 3, the turbulence normal stresses are plotted for the three cases. In these plots, each stress is normalized by the sum of all three, indicating the percent contribution of each to the total kinetic energy. In the unstratified case (Figure 3a), the three stresses contribute about equally to the total energy, but with stratification (Figures 3b and 3c), the magnitude of $\overline{w'^2}$ decreases with respect to the horizontal normal stresses. A low frequency oscillation of $\overline{w'^2}$ may be seen in Figures 3b and 3c, at approximately twice the Brunt-Vaisala frequency (at N=0.045, the Brunt-Vaisala period = 140 time units, and at N=0.0915, the Brunt-Vaisala period = 69 time units). The normalized bouyancy flux (Figure 4) also oscillates at similar frequencies.

Sample three-dimensional averaged energy spectra are plotted in Figure 5. These show the spectral energy for each of the turbulence normal stresses for the moderately stratified case (N=0.045). The plots are at three separate times, corresponding to 0%, 28%, and 57% of a Brunt-Vaisala period. At the later times, the energy in the vertical velocity is seen to decrease both in the larger and smaller length scales relative to the horizontal velocities.

Although the computed results for this compressible test case cannot be directly compared to the results from incompressible calculations reported in the literature, the qualitative trends were judged to be similar and therefore these results were adequate for the characterization feasibility study.

Postprocessing of Results

CHASE Structure

The objective of the program CHASE is to assist a human researcher in analyzing large amounts of data by examining the behavior of the computed flow quantities. This procedure is automated so that large amounts of data can be analyzed or filtered quickly and preliminary results can be found. Once these results are isolated, the researcher can concentrate his or her efforts on studying those areas of particular interest.

The first task for the program, once presented with a large amount of data, is to organize it in some fashion so that if certain trends in the data exist, they will be easy to identify. This organization is accomplished in the following way. Let a flow variable of interest be called F, and the task at hand is to see how it is related to three additional variables, called Q1, Q2, and Q3. This data should be organized so it can be seen how F

varies with Q1 as Q2 and Q3 are held constant. This is then repeated for different constant values of Q2 and Q3, to see what effect Q2 and Q3 have on the relationship between F and Q1. Then the process is repeated again with F vs. Q2 as a function of Q1 and Q3, etc. If these functions are plotted, the dependence of F on Q1 is determined by looking at the shape of the plotted curve. Does F(Q1) monotonically increase or decrease, or does it oscillate several times? Does the curve look random or does it have some sort of order to it? It can easily be determined whether the functional relationship between F and Q1 is consistent regardless of the values of Q2 and Q3 or whether the function is highly dependent upon the values of Q2 and Q3.

Multiple data units are provided as input to CHASE. Each data unit is comprised of a value of Q1, Q2, and Q3 along with the associated value of F. Since these data units are computed at representative times and each Q is varying with time, then typically there will not be more than one value of Q1 that can be associated with a fixed Q2 and Q3. Therefore, an approximation must be made that over a small range of values, Q2 or Q3 may be regarded as constant. The program takes the minimum and maximum values of Q2 and Q3, and divides each range of values into four equal subranges. Within each subrange, Q2 (or Q3) may be regarded as having a low, medium-low, medium-high, or high value, relative to its own minimum and maximum. Then, the approximation that Q2 and Q3 are constant within each subrange is made, and F vs. Q1 is found within each subrange. The combination of a Q2 subrange and a Q3 subrange is called a region, so for instance F vs. Q1 can be found for the region where Q2 is within the low subrange and Q3 is within the medium-high subrange.

Examples of these types of relationships are shown in Figure 6. In this example, F is the log of the density spectral energy $E_{\rho\rho}$, and Q1 = log(wavenumber), Q2 = the Brunt-Vaisala frequency, and Q3 = time. In Figure 6, $E_{\rho\rho}$ is plotted vs. Q3 (time), with Q1 (wavenumber) and Q2 (N) held constant in each subplot. Each region is numbered from 1 to 16. The mechanics of CHASE include the definition of the regions for each variable, the assignment of each data unit to the appropriate region, and the computations of $\Delta F/\Delta Q$ within each region. CHASE also has the capability of checking to see if there exists a dependence upon Q2 in a subrange where Q2 is assumed to be constant. If so, a recommendation to further subdivide that range is made.

Once the regions are found, then CHASE attempts to assign a simple function relationship to the data within each region. At present, the only functional forms programmed into CHASE are "increase" or "decrease," meaning that F data monotonically increases or decreases with Q, "convex" or "concave," meaning that either F increases and then decreases with Q or F decreases and then increases with Q, "null" or "flat," meaning that there is insufficient data within a region or that the data is constant in Q, and "oscillate," which means that the function F vs. Q has more than one local maxima or minima. This functional form, or "trend," is found for each region.

It was apparent after performing the Navier-Stokes calculations that filtering to eliminate the high frequency scatter would be required before the data could be processed by CHASE. A source of this scatter is the presence of high frequency sound waves (with a period of 2π) that are not adequately dissipated. Since CHASE finds functional forms by determining the number of local maxima and minima, it would misinterpret data with a lot

of scatter (for instance, in Figures 3-4). A fourth-order filter to the data was used, with the method of periodic continuation used to treat the boundary points.

The data manipulation portion of the program is fairly straightforward, and it would not be difficult in the future to include more sophisticated functional forms for CHASE to check within each region. Another future improvement could be the inclusion of curve fits within each region, in order to get an algebraic functional form. After this organization of the data is completed, the remainder of the program resembles an "expert system" in that rules that draw conclusions from the data are derived from how a human expert would solve the problem, and these rules are programmed into the system.

The original objective of CHASE was to evaluate how a computed flow field is dependent upon certain initial conditions, such as the numerical boundary conditions.[1] Thus, the rules initially contained in the expert system rule base were designed to look for the greatest sensitivity of the output on the input. These rules were not entirely applicable to the present problem, however. They may be sufficient for looking at how a quantity such as the spectral energy may depend upon independent variables such as in the example above, but when comparing two time-dependent quantities (F and Q1) with each other, additional rules are needed. Therefore, a substantial effort in the Phase I work was devoted to adding more rules to the expert system to deal with a wider variety of comparisons. An objective of this work was to demonstrate whether rules can be devised that are more appropriate for the type of data being evaluated. For instance, from a review of the literature, certain conclusions about the processes in a stratified turbulent flow field may be drawn. A few of these conclusions were selected to be a test case for the modified version of CHASE. These conclusions (taken from References 2, 3, 4, and 6) are listed here:

1. For unstratified flow, the energy cascades from large to small scales over a broad band of wavelengths. In stratified flow, once the turbulence has collaped, the energy transfer occurs from small scales to large scales, and is limited to the lower wavenumbers. This behavior is consistent with the energy transfer in two-dimensional turbulence decay.

2. The spectra of the turbulence kinetic energy and the bouyancy flux peak at the same low wavenumber, but the bouyancy flux has more energy at higher wavenumbers.

3. The onset of bouyancy effects occurs when $(\overline{\rho' \rho'})^{1/2}/(\partial \overline{\rho} / \partial z) = 0.85\ L_{oz}$, and the turbulence becomes extinct when $L_{oz} = B\ L_k$, where B is approximately 8 - 10. The extinction of turbulence is also characterized by the bouyancy flux going to zero (no vertical mixing is taking place).

4. The turbulence collapse time is distinct and occurs at approximately 95% of a Brunt-Vaisala period and a Froude number of 0.25. This time also coincides with the time when L_{oz} and L_k are equal, and possibly coincides with a temporary jump in the Froude number.

5. The vertical length scales are limited by the stratification, while the horizontal scales' growth are enhanced by the stratification.

6. A comparison of horizontal and vertical one-dimensional spectra show that the vertical energy is much higher than the horizontal energy at high wavenumbers.

7. The kinetic energy spectral transfer is inhibited by stratification, but the potential energy transfer is enhanced.

Rule Bases

From an investigation of the conclusions listed above, it was determined that rule bases covering three different aspects of the data would be required. These rule bases are described below:

1. Comparison Rule Base

This rule base is used for conclusions 2, 5, and 6 above. The purpose of this rule base is to compare two quantities against each other as a function of two independent variables. It should be able to determine whether one flow quantity is greater than another and under what conditions this is true. The rule base should also be able to look at each dependent variable individually to determine its functional dependence on the independent variables.

The information required for this task is

a) F1 vs. Q1, Q2

b) F2 vs. Q1, Q2

c) F1 vs. F2, Q1, Q2.

For a) and b), F would be looked at as a function of one of the Q's with the other Q held fixed. Therefore there would be four regions in the problem, which correspond to the subranges of the Q that is held fixed. Given the information from a) and b), the rules that were programmed into the system were:

1. If the trends of F1 vs. Q1 are the same for all regions (excluding the regions with null data), then the value of Q2 does not affect the functional form of F1 vs. Q1.

(repeat for F1 vs. Q2, for F2 vs. Q1, and for F2 vs. Q2)

2. If the trends of F1 vs. Q1 vary from region to region, then the value of Q2 affects the functional form of the F1 vs. Q1 dependence, and this functional form may be described by the trend found in each of the four regions.

3. If the trends of F1 vs. Q1 are the same for all regions, and the trends of F2 vs. Q1 are the same for all regions, and these two trends are the same, then F1 and F2 are similar functions of Q1. (repeat for Q2)

4. If the trends of F1 vs. Q1 are the same for all regions, and the trends of F2 vs. Q1 are the same for all regions, and these two trends are not equal, then F1 and F2 are difference functions of Q1.

5. If the trends of F1 vs. Q1 are the same for all regions, and the trend is either increase or decrease, and the absolute value of the average slope within a region increases (decreases) by more than 20% when Q2 changes from low to high, then the dependence of F1 on Q1 is strengthened (weakened) as Q2 increases.

6. If the trends of F1 vs. Q1 are the same for all regions, and the trend is either increase or decrease, and the absolute value of the rms slope within each region increases (decreases) by more than 20% when Q2 changes from low to high, then the nonlinearity of F1 vs. Q1 is strengthened (weakened) as Q2 increases.

7. If the trends of F1 vs. Q1 are the same for all regions, and the trend is either concave or convex or oscillate, and the absolute difference between the maximum and minimum values of F1 within a region increases (decreases) by more than 20% when Q2 changes from low to high, then the dependence of F1 on Q1 is strengthened (weakened) as Q2 increases.

8. If the trends of F1 vs. Q1 are the same for all regions, and the trend is oscillate, and the average spacing between peak value within a region increases (decreases) by more than 20% when Q2 changes from low to high, then the frequency of F1 vs. Q1 is increased (decreased) as Q2 increases.

With the information from c) above, the program can then compare F1 and F2. There are now 16 regions of interest, corresponding to each combination of one of the four Q1 subranges with one of the four Q2 subranges. These rules are:

9. If the instances where F1 is higher than F2 are greater than the instances where F2 are higher than F1 within any region, then F1 is greater than F2 within that region.

10. If F1 is greater than F2 in all regions, then F1 is greater than F2 independently of Q1 and Q2.

11. If there are more regions where F1 is greater than F2, but F1 is not greater than F2 independently of Q1 and Q2, then F1 is greater than F2 dependent upon the values of Q1 and Q2.

12. If F1 is greater than F2 in regions 1-4, and F2 is greater than F1 in regions 13-16 (see Figure 6), then F1 is greater than F2 for low Q2 independently of Q1, and F2 is greater than F1 for high Q2 independently of Q1.

2. Sensitivity Rule Base

This rule base is used for conclusions 1 and 7 above. The purpose of this rule base is to look at a dependent variable and determine its relationship to other variables in the

problem. For the conclusions given above, the additional variables (Q's) in the problem are true independent variables, namely wavenumber, time, and stratification. Although there would be no difficulty in programming the code to look at more than three dependent variables, for this problem only three variables are of interest. With three Q's there are 16 regions of interest, corresponding to the subrange values of two of the Q's while F_1 is being studied as a function of the third Q.

The information required for this task is

a) F vs. Q1, Q2, Q3.

This rule base consists of essentially two rules, which determine what the values of Q2 and Q3 are when F is most/least sensitive to Q1 (repeated for other Q's). This information can then be used to determine relationships such as are required for the above conclusions, such as the effect of stratification on how much energy exists in various wavenumbers as time changes.

3. Events Rule Base

This rule base was written to be a generalization of what would be required to draw conclusions 3 and 4 above. The objective of this rule base is to determine if there are any correlations between F1 and F2 at a particular time. These correlations are said to have taken place if F1 has an "event" at a particular time, and F2 maintains a constant value at that time. For instance, if F1 vs. time shows a marked occurrence at a particular time at one stratification, and the same occurrence at a different time at another stratification, and if F2 during the first event is approximately equal to F2 at the second event, then F2 is said to have a characteristic value correlated to the F1 event. The two types of "events" that are currently considered in the program are the times when F1 significantly departs from its unstratified value, and the times when F1 has a zero crossing.

The information required for this rule base is

a) F1 vs. Q1, Q2

b) F2 vs. Q1, Q2

The departure of F1 from its unstratified value may be computed by letting Q1 equal time and Q2 equal the Brunt-Vaisala frequency. Then, $\Delta F1(Q1) = F1(Q1,Q2=a) - F1(Q1,Q2=0)$. The value of Q1 where $\Delta F1$ first increases above 10% is considered to be the characteristic time where stratification first affects F1. If the event to be considered is a zero crossing, then the time when F1 becomes zero is straightforward to compute, and that is the characteristic time. Next, the value of F2 at Q1=a and Q2=characteristic time for a is compared with the value of F2 at Q1=b and Q2=characteristic time for b. If F2 differs by no more than a certain percentage (approximately 10%), then F2 is said to have a characteristic value that correlates with the F1 event.

CHASE Computational Requirements

CHASE was originally written in the artificial intelligence language Prolog. Although Prolog is well suited to the rule base section of the program, it was inefficient at performing the numerical computations that are required for the data manipulation part of the program. Prolog cannot handle large number sets, and it is very memory intensive since it is a recursive language. Another disadvantage is that it could not be run on either the Cray or a VAX front end, as these machines typically do not have Prolog compilers.

During the course of this contract it was decided to rewrite the code in Fortran. This solved many of the computational problems that existed with the Prolog version. Fortran can easily perform the required algebraic manipulations, and may be run on either the Cray or a VAX. The programming of the rule base was not too difficult in Fortran, since the rules described above are only one level deep. That is, the program performs a calculation, and depending upon the results of that calculation, the program outputs a conclusion. However, it is anticipated that for future extensions to CHASE, the rule base will be several levels deep, meaning that the conclusion from a computation will be used to form further conclusions, and so on. In that case, Fortran might become too inefficient for the task.

For future work, CHASE may be rewritten again in C. C seems to be the optimal language for this task, since it is well suited to both numerical calculations and also has functions to manage text strings. Another advantage to C is that it may be run on a Cray under the Unicos operating system, so there will be no difficulty in transferring data from the atmospheric code to CHASE.

In any language, CHASE is a small code compared to the fluid flow simulation, and it has no special computational requirements. The Fortran version run time is on the order of a few seconds on a VAX. CHASE has a friendly user interface which interactively queries the user as to which rule base and which flow variables are of interest.

Results and Discussion

Comparison Results

Test cases for the comparison rule base were run in order to verify conclusions 2, 5, and 6. The most straightforward comparison is between the horizontal and vertical length scales, L_{hmv} and L_{vmv}. In this problem, F1 = L_{vmv}, F2 = L_{hmv}, Q1 = time, and Q2 = N. Figure 7 shows how L_{vmv} varies with each Q. In these plots, L is shown vs. one of the Q's, while the other Q is divided into four subranges; thus there are four regions in each plot.

The output from CHASE for this example was:

"The value of N does not affect the functional form of the L_{vmv} vs. time dependence."
"The trend for L_{vmv} vs. time is either convex or concave or oscillate."
"The value of time affects the functional form of the L_{vmv} vs. N dependence, and the *functional form of L_{vmv} vs. N may be described as*
decrease at low time

concave at medium-low time
concave at medium-high time
increase at high time"

"The frequency of L_{vmv} vs. time is increased as N increases."
"The value of N does not affect the functional form of the L_{hmv} vs. time dependence."
"The trend for L_{hmv} vs. time is either convex or concave or oscillate."
"The trend for L_{hmv} vs. time is oscillate."
"The value of time does not affect the functional form of the L_{hmv} vs. N dependence."
"The trend for L_{hmv} vs. N is either increase or decrease."
"The dependence of L_{hmv} on N is strengthened as time increases."
"The dependence of L_{hmv} on time is strengthened as N increases."
"The frequency of L_{hmv} vs. time is increased as N increases."
"L_{hmv} is greater than L_{vmv} independently of time and N."

Since the horizontal scales are slightly larger than the vertical scales for the unstratified case, the expert system could not draw the conclusion that the stratification enhanced the horizontal scales while limiting the vertical scales (conclusion 5). With that exception, though, the rule base was able to evaluate the correct trends within the results, given the simplicity of the functional forms programmed into the system.

Another example is the comparison of the three-dimensional spectra of the kinetic energy and the bouyancy flux. In this example, F1 = log(E_{uu}), F2 = log($E_{\rho w}$), Q1 = log(wavenumber), and Q2 = N. All the data is at a fixed time (t = 80).

The output from CHASE was:
"The value of N affects the functional form of the E_{uu} vs. κ dependence, and the functional form of E_{uu} vs. κ may be described as
decrease at low N
decrease at medium-low N
null at medium-high N
oscillate at high N"
"The value of κ affects the functional form of the E_{uu} vs. N dependence, and the functional form of E_{uu} vs. N may be described as
increase at low κ
decrease at medium-low κ
decrease at medium-high κ
decrease at high κ"
"The value of N does not affect the functional form of the $E_{\rho w}$ vs. κ dependence."
"The trend for $E_{\rho w}$ vs. κ is either increase or decrease."
"The value of κ affects the functional form of the $E_{\rho w}$ vs. N dependence, and the functional form of $E_{\rho w}$ vs. N may be described as
concave at low κ
decrease at medium-low κ
decrease at medium-high κ
null at high κ"
"E_{uu} is greater than $E_{\rho w}$ independently of κ and N."

Conclusion 2 states that the two spectra should peak at the same low wavenumber. Currently the output from CHASE does not go that far, but from the information presented one could conclude that since the functional form for both E_{uu} and $E_{\rho w}$ vs. κ is "decrease," that the maximum energy occurs at the lowest wavenumber for both. An additional rule for CHASE that determined that E_{uu} decreased faster than $E_{\rho w}$ would be able to conclude that $E_{\rho w}$ has more energy at a higher wavenumber.

The final example for the comparison rule base is the one-dimensional velocity spectra in the vertical and horizontal directions. For this problem, F1 = 1-d $E_{uu}(\kappa_x)$, F2 = 1-d $E_{ww}(\kappa_z)$, Q1 = κ, and Q2 = N. Figures 8 and 9 show the results from this case that CHASE used to draw conclusions, and the output from CHASE was:

"The value of N does not affect the functional form of the E_{uu} vs. κ dependence."
"The trend for E_{uu} vs. κ is either increase or decrease."
"The value of κ affects the functional form of the E_{uu} vs. N dependence, and the functional form of E_{uu} vs. N may be described as
increase at low κ
decrease at medium-low κ
decrease at medium-high κ
decrease at high κ"
"The dependence of E_{uu} on κ is strengthened as N increases."
"The nonlinearity of E_{uu} vs. κ is strengthened as N increases."
"The value of N affects the functional form of the E_{ww} vs. κ dependence, and the functional form of E_{ww} vs. κ may be described as
decrease at low N
oscillate at medium-low N
null at medium-high N
oscillate at high N"
"The value of κ affects the functional form of the E_{ww} vs. N dependence, and the functional form of E_{ww} vs. N may be described as
concave at low κ
convex at medium-low κ
decrease at medium-high κ
increase at high κ"
"E_{ww} is greater than E_{uu} dependent upon the value of κ and N."

The last statement from CHASE provides most of the information that is needed for conclusion 6; however, what is missing is a statement as to which wavenumbers or stratifications lead to the higher vertical energies. These further elaborations to the rule base will be added in future versions of the code.

Sensitivity Results

Several test cases were run to test the sensitivity rule base. These cases investigated the dependence of the spectral energy on the wavenumber, time, and stratification. To verify conclusion 7, the three-dimensional spectral kinetic ($E_{ke} = E_{uu} + E_{vv} + E_{ww}$) and potential energies ($E_{\rho\rho}$) were studied. In these instances, F1 = log(E), Q1 = log(κ), Q2 = time, and Q3 = N. Figure 10 shows the 16 regions associated with each F1 vs. Q plot. In Figure 10a,

$\log(E_{ke})$ is plotted against Q1 (log(wavenumber)) at all 16 combinations of the Q2 (stratification) and Q3 (time) subranges. Figure 10b shows F1 vs. Q2, and Figure 10c shows F1 vs. Q3.

The list of conclusions output by CHASE were:

1. "E_{ke} is more sensitive to wavenumber when time is low."
2. "E_{ke} is more sensitive to wavenumber when N is high."
3. "E_{ke} is least sensitive to wavenumber when time is medium-high."
4. "E_{ke} is least sensitive to wavenumber when N is low."
5. "E_{ke} is more sensitive to N when time is medium-high."
6. "E_{ke} is more sensitive to N when wavenumber is medium-high."
7. "E_{ke} is least sensitive to N when time is medium-high."
8. "E_{ke} is least sensitive to N when wavenumber is low."
9. "E_{ke} is more sensitive to time when N is high."
10. "E_{ke} is more sensitive to time when wavenumber is medium-high."
11. "E_{ke} is least sensitive to time when N is medium-low."
12. "E_{ke} is least sensitive to time when wavenumber is low."

A contradiction seems to occur in the above statements, since E_{ke} is both more sensitive and least sensitive to N when time is medium-high. In Figure 10b, it can be seen that the difference lies in the value of the wavenumber. E_{ke} is least sensitive to N at medium-high time (Q_3) and low wavenumbers (Q_1), and E_{ke} is most sensitive to N at medium-high time (Q_3) and medium-high wavenumbers (Q_1). This functional interdependence between Q_1 and Q_3 would need to be accounted for in later versions of CHASE.

Further understanding of the above conclusions could be made if the statements were rewritten slightly. For instance, if "E_{ke} is more sensitive to time when . . ." were replaced by 'E_{ke} changes more rapidly when . . .," more insight into the processes could be gained. Another more useful way to rephrase a conclusion might be "The kinetic energy in the large scales is least affected by the stratification" rather than "E_{ke} is least sensitive to N when wavenumber is low," Statements could also be combined, such as writing "The kinetic energy in the small scales changes more rapidly as N increases" instead of the separate statements "E_{ke} is more sensitive to time when wavenumber is medium-high" combined with "E_{ke} is more sensitive to time when N is high." The current version of CHASE is written to be as general as possible, but it would not be difficult to extend the rule base in future versions to account for these clarifications.

The analysis was repeated for the density spectral energy $E_{\rho\rho}$. Figure 11 shows the corresponding functional dependencies for this case. The conclusions made by CHASE were:

1. "$E_{\rho\rho}$ is more sensitive to wavenumber when time is low."
2. "$E_{\rho\rho}$ is more sensitive to wavenumber when N is high."
3. "$E_{\rho\rho}$ is least sensitive to wavenumber when time is medium-high."
4. "$E_{\rho\rho}$ is least sensitive to wavenumber when N is high."
5. "$E_{\rho\rho}$ is more sensitive to N when time is low."
6. "$E_{\rho\rho}$ is more sensitive to N when wavenumber is medium-high."

7. "$E_{\rho\rho}$ is least sensitive to N when time is medium-high."
8. "$E_{\rho\rho}$ is least sensitive to N when wavenumber is low."
9. "$E_{\rho\rho}$ is more sensitive to time when N is high."
10. "$E_{\rho\rho}$ is more sensitive to time when wavenumber is medium-high."
11. "$E_{\rho\rho}$ is least sensitive to time when N is low."
12. "$E_{\rho\rho}$ is least sensitive to time when wavenumber is medium-high."

Although 10. and 12. above seem to conflict, the missing information that 10. is true for high N and 12. is true for low N would resolve the issue.

At present CHASE is not programmed to compare the results from two sensitivity studies, but a manual comparison of the above results shows the following: $E_{\rho\rho}$ is affected earlier by the stratification, and E_{ke} is most strongly affected by the stratification at later times; $E_{\rho\rho}$ changes less with time at zero stratification than E_{ke} does; however, with stratification, $E_{\rho\rho}$ decays more rapidly with time than E_{ke} does (in support of conclusion 7); and at high stratification, it can be seen that the smaller scales decay more rapidly with time than the larger scales, thus verifying conclusion 1.

Even though CHASE does not at present deduce the further conclusions from the basic ones, once the thought processes are identified for how to make those further conclusions, it will not be difficult to program the rules to draw those same conclusions. The necessary modifications to conclude more sophisticated relationships from the data will be performed in future work.

Events Results

Two test cases were run to test the events rule base. The first case was to see if the onset of stratification occurs when L_{tr}/L_{oz} has a characteristic value (from conclusion 3, since $L_{tr} = 0.5*(\overline{\rho'\rho'})^{1/2}/(\partial\overline{\rho}/\partial z)$). F1 was taken to be the horizontal length scale L_{hmv}, and when this length scale departs from the unstratified value was taken to indicate the onset of bouyancy. In this example, L_{oz} was defined as $(\overline{w'^2})^{1/2}/N$, as given in Reference 7. This bouyancy length scale is defined to be the vertical distance travelled by a fluid particle as it converts its kinetic energy into potential energy. The definition of this length scale given in the input/output quantities section is made after approximating that the turbulent kinetic energy (tke) is proportional to $\overline{w'^2}$ and the dissipation ε is proportional to $(tke)^{3/2}$ divided by the length scale. As stated by Stillinger,[7] this second definition of L_{oz} will be inaccurate if the kinetic energy includes contributions from the internal wave field. Since the first definition is more accurate, that is the one that was used in this case.

With F1 = L_{hmv}, F2 = L_{tr}/L_{oz}, Q1 = time, and Q2 = N, CHASE came to the conclusion that:

"L_{hmv} has an event that depends upon the stratification at time 33.34 for N = 0.045 and at time 28.31 for N = 0.0915. L_{tr}/L_{oz} has a characteristic value of 2.3828 at that time."

Figure 12 shows the time evolution of L_{hmv} and L_{tr} and L_{oz} for the unstratified and two stratified cases. It can been seen that the rapid decay of the length scales clearly

depends upon the stratification. In conclusion 3 above, it was stated that the onset of bouyancy occurs when $(\overline{\rho'\rho'})^{1/2}/(\partial\overline{\rho}/\partial z) = 0.85\ L_{oz}$ (Ref. 2), but in this calculation, $(\overline{\rho'\rho'})^{1/2}/(\partial\overline{\rho}/\partial z) = 1/2\ L_{tr} = 1.1914\ L_{oz}$, which differs by forty percent from the reported value in the literature. The program was able to accurately predict the correct value from the current data set, as can be seen from Figure 12.

The second test case for the events rule base was to correlate the Froude number with the time when the bouyancy flux goes to zero. This test case comes from a combination of conclusions 3 and 4, where the bouyancy flux going to zero indicates an extinction of turbulence. In this problem, F1 is the normalized bouyancy flux, F2 is the Froude number, Q1 is time, and Q2 is N. The output from CHASE read:

"The bouyancy flux equals zero at time 65.00 for N = 0.045 and time 27.51 for N = 0.0915. At these times the Froude number has a characteristic value of 0.1508."

As can be seen in Figure 13, which shows the Froude number vs. time, the Froude number changes very little at later time, so this conclusion was not difficult for the program to make. The value of the Froude number from this computation was lower than that predicted in conclusion 4 for the turbulence collapse time. The times when the bouyancy flux went to zero were approximately forty-five percent of a Brunt-Vaisala period for both stratifications, and it is expected that these normalized time periods would correlate for the extinction of turbulence. The normalized times do not correlate for the onset of bouyancy effects, but that is not surprising since the characteristic time scale due to bouyancy should have little meaning before bouyancy affects the flowfield.

As can be seen from the current calculation results, L_{oz} and L_k do approach each other in magnitude at approximately one B-V period, as stated in conclusion 4. However, this time does not coincide with the zero crossing of the bouyancy flux. When the ratio L_{oz}/L_k was used for F2, the program could not find a characteristic value, since $L_{oz}/L_k = 4.14$ @ time = 65.0, N = 0.045, and $L_{oz}/L_k = 2.79$ @ time = 27.5, N = 0.0915.

Conclusions and Future Recommendations

A data postprocessor/expert system was written to assist in the data analysis task for numerical fluid simulations. This program, CHASE, has the ability to organize the data so that relationships among the flow variables become apparent, and also is able to form judgments about the data based on those relationships. Since the program is automated, it has the potential to quickly analyze large amounts of data from a flow simulation, making this tool a useful assistant to the fluid mechanics investigator.

The expert system rule base developed for this work was general enough so that data from any flow calculation may be used as input. However, the development of each of the rule base tasks was guided by the stratified turbulence calculation, so the addition of further rule bases for additional tasks is a possibility for future work. The user of the code then chooses the particular task in which he is interested.

In particular, in the future it would be of great interest to develop rule bases for two tasks. First is the task of choosing which flow quantities are of interest, so that they can be computed and stored at representative time steps during the flow calculation. The second task is the choice of which flow quantities, out of a given list of variables, should be studied as functions of which other variables, and how many of these other variables should be used in order to document a complete interaction phenomena.

The first task is possibly the more difficult of the two. Useful results from a correlation or sensitivity study will depend upon the choice of the correct variables for comparison. For example, in the first events test case the important parameter was the ratio of two length scales, rather than one of the length scales alone. There are certain rules that investigators use to determine what the important parameters of a flow are. Examples are that all quantities of importance should be nondimensional, and that only like quantities should be compared with each other (length scales to length scales rather than length scales to energy). These two rules may be used in the program to considerably narrow down what might otherwise be an exhaustive search for appropriate variables. If the problem at hand is to find particular quantities that reach a characteristic value at some time in the flow evolution, then only ratios of two like quantities, with each representing a characteristic physical quality of the flow, should be chosen. The same principle should also apply to the sensitivity studies. The results of the sensitivity study to verify conclusion 7 could have been determined by using the ratio of E_{ke} to $E_{\rho\rho}$ instead of each quantity separately. In future work, discussions with scientists who are familiar with evaluating these flows should take place in order to form a set of rules that may be used to narrow down these choices of variables.

The second task also requires expert knowledge. For instance, in the sensitivity study, three quantities were treated as the independent variables, but in some cases, it may be more appropriate to use five. Extending the rule base to deal with more than three variables would be straightforward, but the decision of how many variables to use for a certain situation requires a decision process. One possibility would be to preselect variables by performing a quick analysis of all possible choices, and then complete the more detailed analysis on the most promising of these choices.

Other issues will also have to be studied in future work. One problem is the possibility that phantom relationships would be found by the program, that is, CHASE would create a relationship between unrelated quantities. Another problem to address is that of the need to filter the data. It would have to be determined how much filtering is required without losing information that is valuable. Some distinction between noise and representative data would have to be made.

A third problem concerns the probability that a certain conclusion is true. In the events rule base, an error bracket of 10% was used when determining whether two quantities are equal or deviate from each other. This value of 10% was chosen arbitrarily. Future rules should be written so that several error brackets can be used, and the probability that the conclusion is correct would be provided to the user dependent upon the error involved.

In summary, there are many research issues to be addressed in future work, but the results of this Phase I study indicate that the concept is feasible and that a successful production version of this code can be written.

References

1. Rodman, L. C., "A Characterization and Search Technique for Unsteady Flow Control Problems," AIAA-90-3102, AIAA 8th Applied Aerodynamics Conference, Portland, OR, August 1990.

2. Itsweire, E. C. and Helland, K. N., "Spectra and Energy Transfer in Stably Stratified Turbulence," J. Fluid Mech., Vol. 207, 1989, pp. 419-452.

3. Riley, J. J., Metcalfe, R. W., and Weissman, M. A., "Direct Numerical Simulations of Homogeneous Turbulence in Density-Stratified Fluids," Proceedings of the American Institute of Physics Conference on Nonlinear Properties of Internal Waves, Vol. 76, 1981, pp. 79-112.

4. Metais, O. and Herring, J. R., "Numerical Simulations of Freely Evolving Turbulence in Stably Stratified Fluids," J. Fluid Mech., Vol. 202, 1989, pp. 117-148.

5. Kwak, D., Reynolds, W. C., and Ferziger, J. H., "Three-Dimensional Time Dependent Computation of Turbulent Flow," Report No. TF-5, Thermosciences Division, Department of Mechanical Engineering, Stanford University, 1975. (Also NASA-CR-143347)

6. Riley, J. J., "A Review of Turbulence in Stably-Stratified Fluids," Seventh Symposium on Turbulence and Diffusion, Amer. Meteorol. Soc., Boulder, CO, November 1985.

7. Stillinger, D. C., Helland, K. N., and van Atta, C. W., "Experiments on the Transition of Homogeneous Turbulence to Internal Waves in a Stratified Fluid," J. Fluid Mech., Vol. 131, 1983, pp. 91-122.

WRITTEN PUBLICATIONS

1. Rodman, L. C.: Meteorological Model Analysis for Numerical Weather Prediction. Abstract submitted to the Ninth Conference on Numerical Weather Prediction, Denver, Colorado, October 1991.

PROFESSIONAL PERSONNEL

Dr. Laura C. Rodman
Dr. Robert E. Childs

INTERACTIONS

No significant interactions have taken place during this work.

DISCOVERIES

No new discoveries or patents have resulted from this work.

bouyancy flux	$\frac{g}{\rho_o}\ \overline{\rho' w'}$
normalized bouyancy flux	$\frac{\overline{\rho' w'}}{\sqrt{\overline{\rho' \rho'}}\ \sqrt{\overline{w' w'}}}$
Ozmidov length scale	$L_{oz} = \left[\frac{\varepsilon}{N^3}\right]^{1/2}$
Kolmogorov length scale	$L_k = \left[\frac{\nu^3}{\varepsilon}\right]^{1/4}$
Taylor microscales (horizontal)	$L_{hmv} = \frac{\sqrt{\overline{u' u'}}}{\sqrt{\overline{\left[\frac{\partial u'}{\partial x}\right]^2}}}$ $L_{hmr} = \frac{\sqrt{\overline{\rho' \rho'}}}{\sqrt{\overline{\left[\frac{\partial \rho'}{\partial x}\right]^2}}}$
(vertical)	$L_{vmv} = \frac{\sqrt{\overline{w' w'}}}{\sqrt{\overline{\left[\frac{\partial w'}{\partial z}\right]^2}}}$ $L_{vmr} = \frac{\sqrt{\overline{\rho' \rho'}}}{\sqrt{\overline{\left[\frac{\partial \rho'}{\partial z}\right]^2}}}$
horizontal velocity integral scale	$L_{hiv} = \int_0^{2\pi} \frac{\overline{u'(x+\Delta x)\, u'(x)}}{\overline{u' u'}}\, d(\Delta x)$
vertical velocity integral scale	$L_{viv} = \int_0^{2\pi} \frac{\overline{w'(z+\Delta z)\, w'(z)}}{\overline{w' w'}}\, d(\Delta z)$
density turbulent	$L_{tr} = \frac{2g\sqrt{\overline{\rho' \rho'}}}{\rho_o N^2}$

Table 1.- Output flow quantities computed by TMRC.

Froude number	$Fr = \frac{\sqrt{\overline{u'u'}}}{N L_{viv}}$
3-d average spectral energy	$E_\phi(k)\ \Delta k = \frac{1}{N_{shell}} \sum \hat{\phi}(k)\hat{\phi}^*(k)$
$k = \sqrt{k_1^2 + k_2^2 + k_3^2}$	
2-d horizontal energy	$E_\phi(k_h)\ \Delta k = \frac{1}{N_z} \sum \frac{1}{N_{disc}} \sum \hat{\phi}(k_h, z)\hat{\phi}^*(k_h, z)$
$k_h = \sqrt{k_1^2 + k_2^2}$	
1-d vertical energy	$E_\phi(k_3)\ \Delta k = \frac{1}{N_x N_y} \sum \hat{\phi}(x, y, k_3)\ \hat{\phi}^*(x, y, k_3)$
1-d horizontal energy	$E_\phi(k_1)\ \Delta k = \frac{1}{N_z N_y} \sum \hat{\phi}(k_1, y, z)\ \hat{\phi}^*(k_1, y, z)$

where $\hat{\phi}$ = Fourier transform of: u', v', w', ρ', $\rho'w'$,

turbulence statistical quantities: $\overline{u'u'}$, $\overline{v'v'}$, $\overline{w'w'}$, $\overline{\rho'\rho'}$, $\overline{\rho'u'}$, $\overline{\rho'v'}$, $\overline{\rho'w'}$,

$$k.e. = \frac{1}{2}\left[\overline{u'u'} + \overline{v'v'} + \overline{w'w'}\right], \quad p.e. = -\frac{1}{2}\frac{g}{\rho_o}\left|\frac{\partial \bar{\rho}}{\partial z}\right|^{-1} \overline{\rho'\rho'}$$

velocity derivative skewness

$$\frac{\overline{\left[\frac{\partial u'}{\partial x}\right]^3}}{\overline{\left[\frac{\partial u'}{\partial x}\right]^2}^{3/2}} \qquad \frac{\overline{\left[\frac{\partial w'}{\partial z}\right]^3}}{\overline{\left[\frac{\partial w'}{\partial z}\right]^2}^{3/2}}$$

Table 1.- continued.

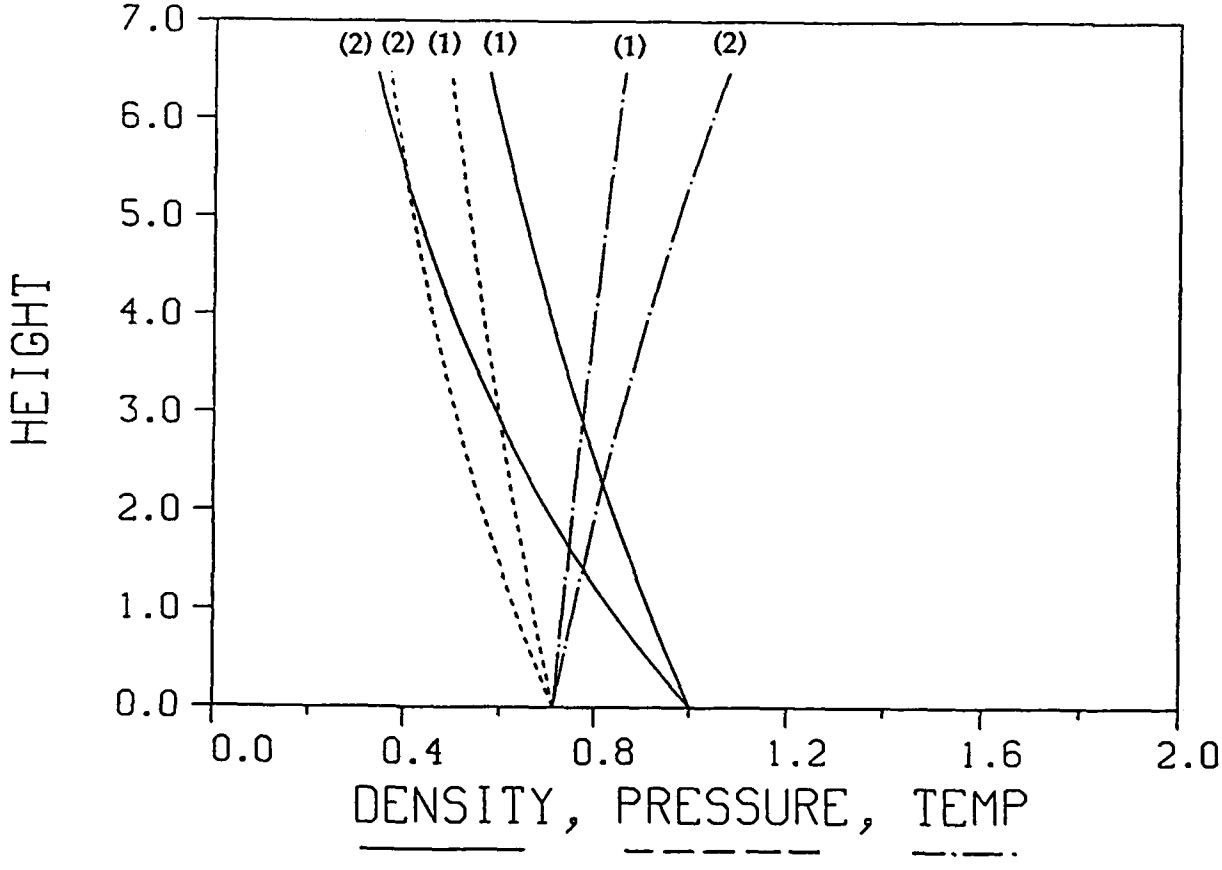

Figure 1.- Density, pressure, and temperature vs. height for case 1 (N=0.045, g=0.045) and case 2 (N=0.0915, g=0.09).

(a)

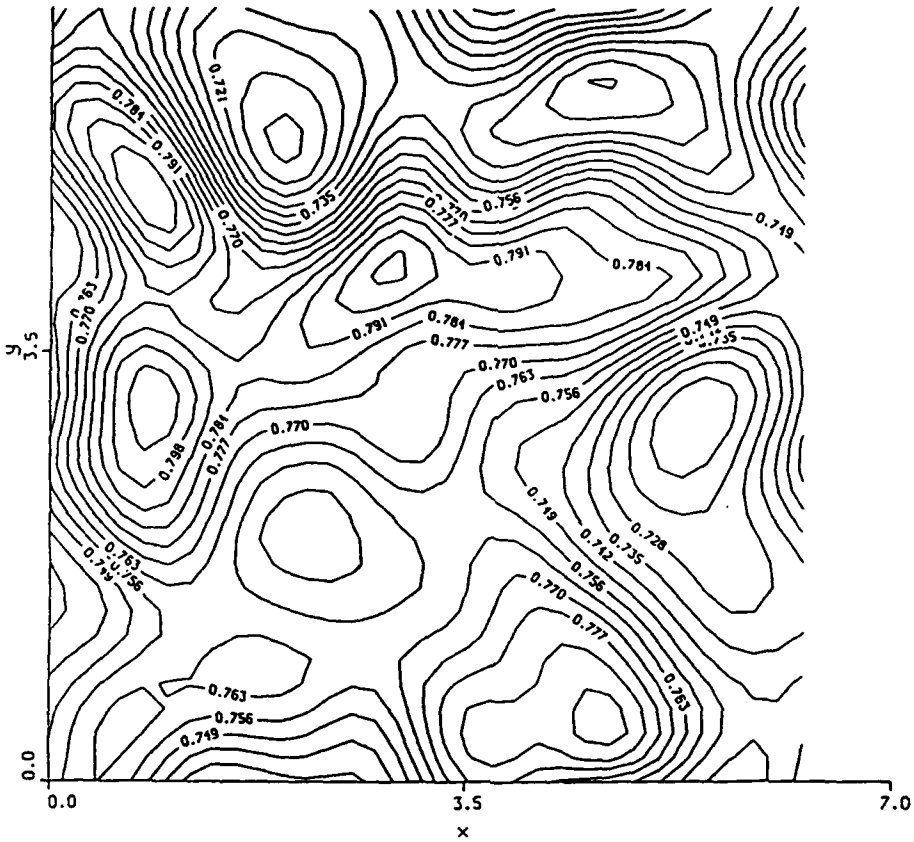

(b)

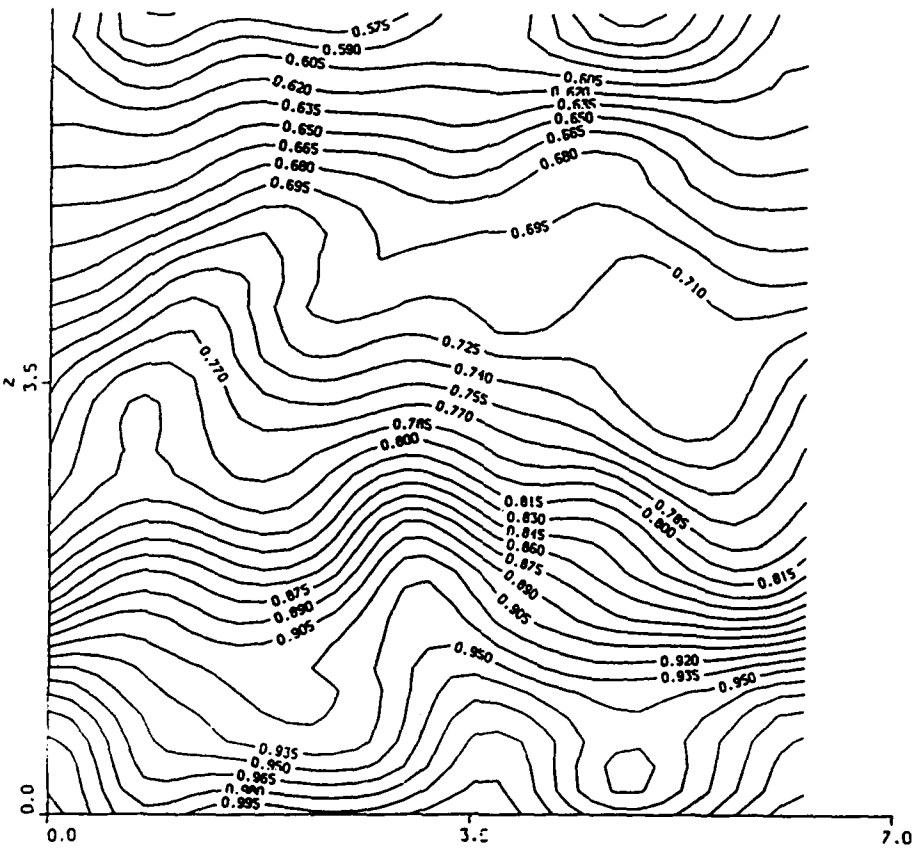

Figure 2.- Density contours for case 1 (N=0.045, g=0.045) at time=41.5 (30% of one Brunt-Vaisala period). (a) horizontal plane, (b) vertical plane.

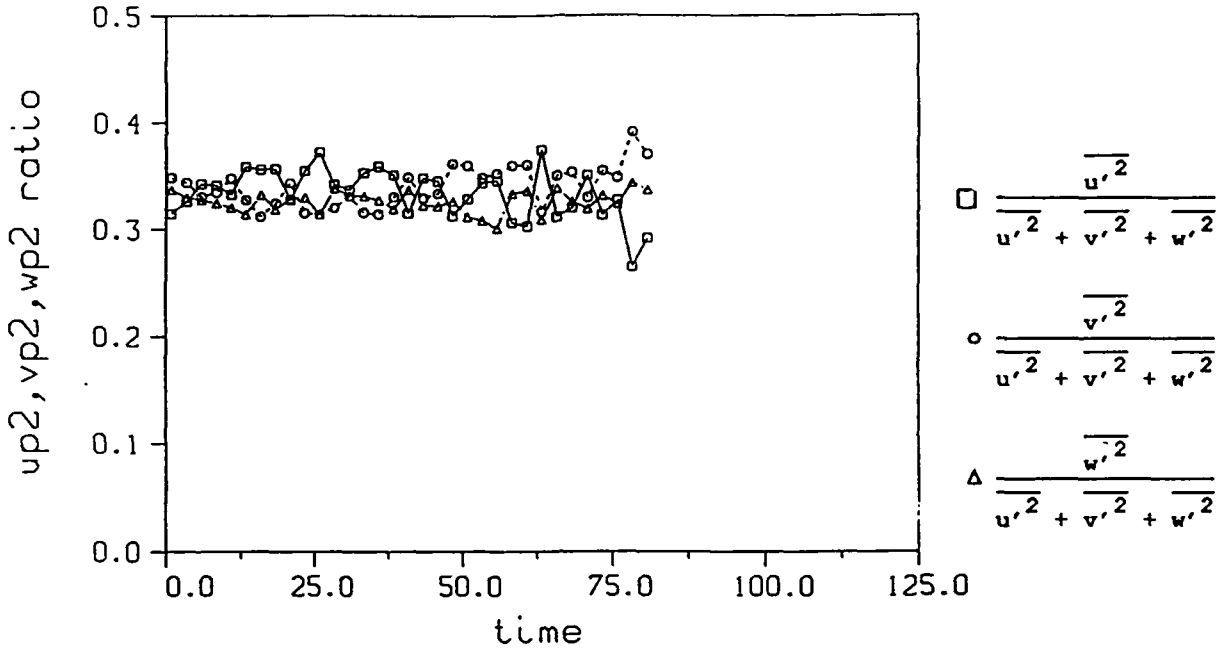

(a)

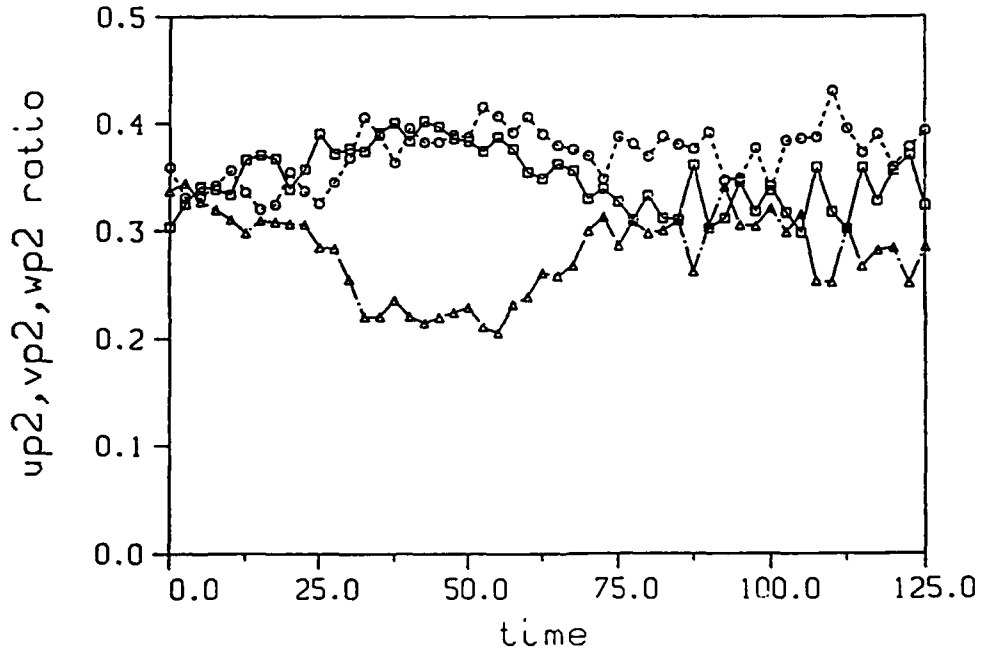

(b)

Figure 3.- Ratio of individual normal stress components to total normal stress vs. time. (a) Unstratified case, (b) Stratified (N=0.045, g=0.045, B-V period = 140), (c) Stratified (N=0.0915, g=0.09, B-V period = 69).

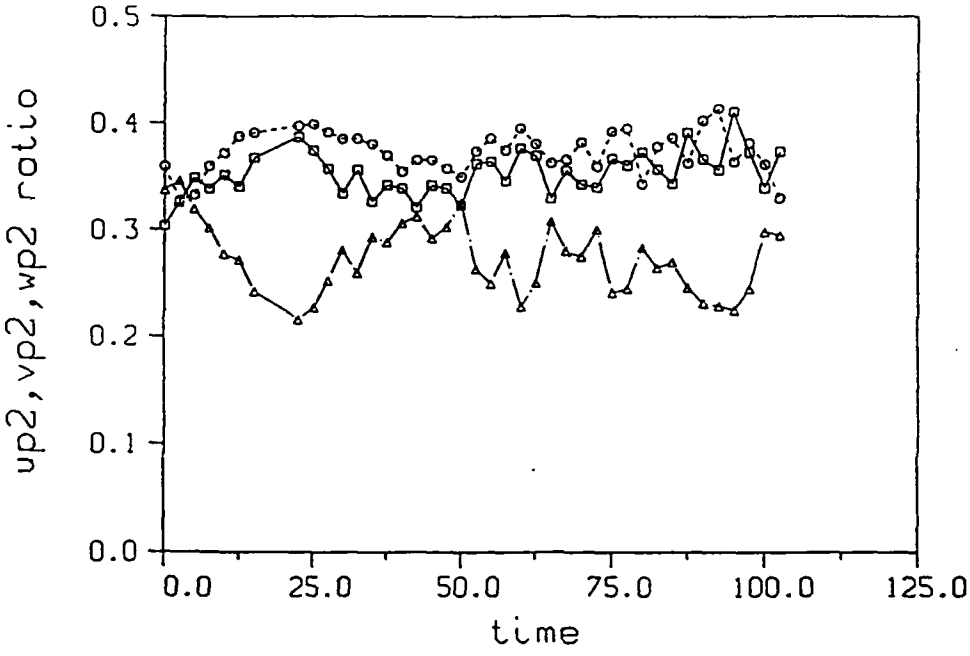

(c)

□ $\dfrac{\overline{u'^2}}{\overline{u'^2} + \overline{v'^2} + \overline{w'^2}}$

o $\dfrac{\overline{v'^2}}{\overline{u'^2} + \overline{v'^2} + \overline{w'^2}}$

Δ $\dfrac{\overline{w'^2}}{\overline{u'^2} + \overline{v'^2} + \overline{w'^2}}$

Figure 3.- continued.

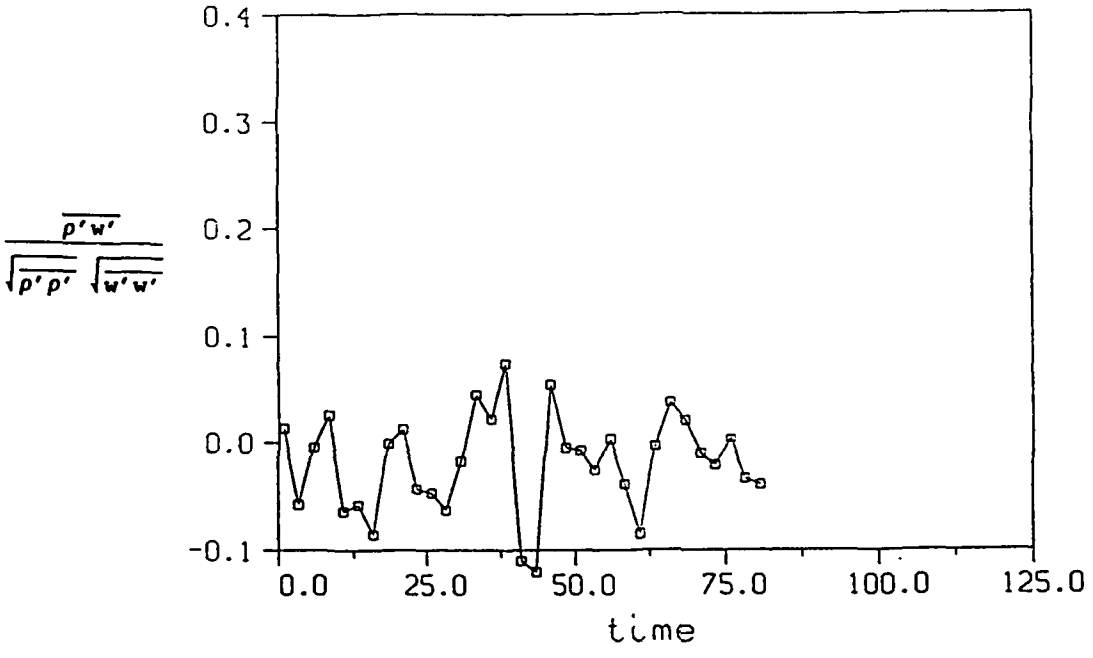

(a)

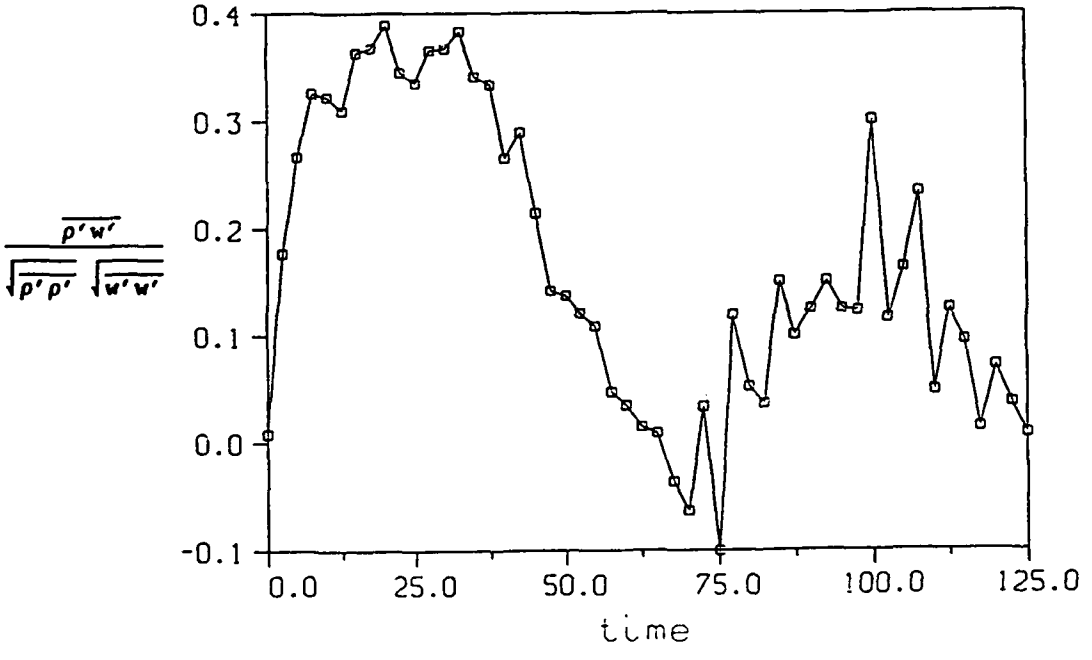

(b)

Figure 4.- Normalized bouyancy flux vs. time. (a) Unstratified case, (b) Stratified (N=0.045, g=0.045, B-V period=140), (c) Stratified (N=0.0915, g=0.09, B-V period=69).

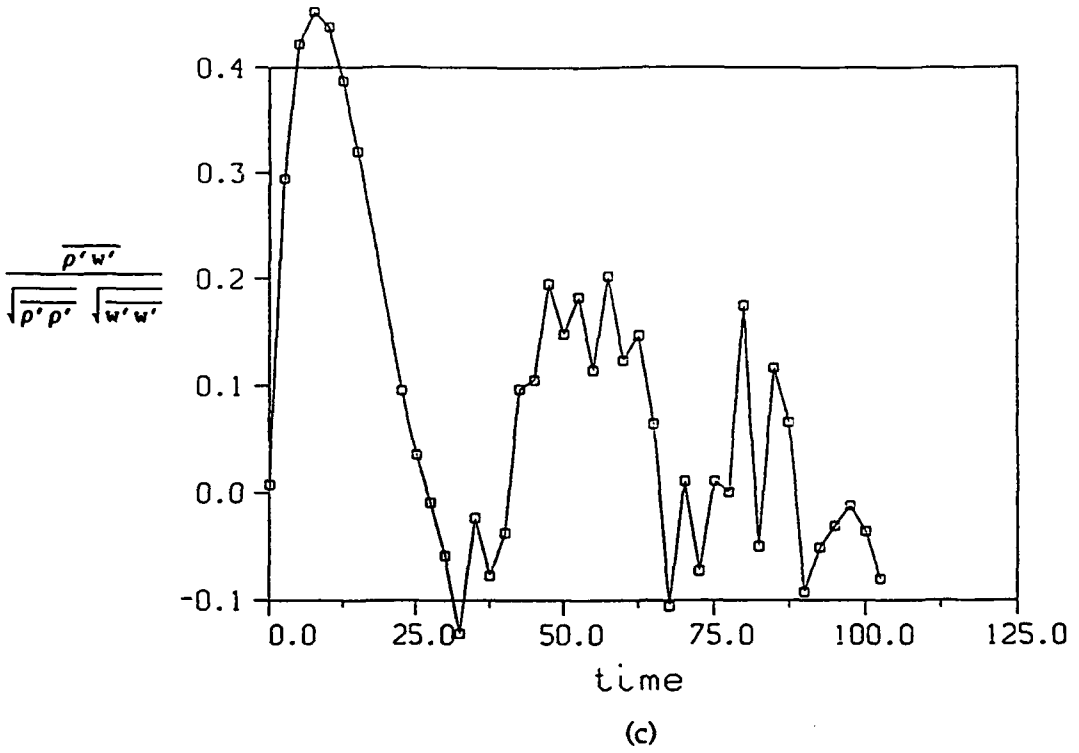

Figure 4.- continued.

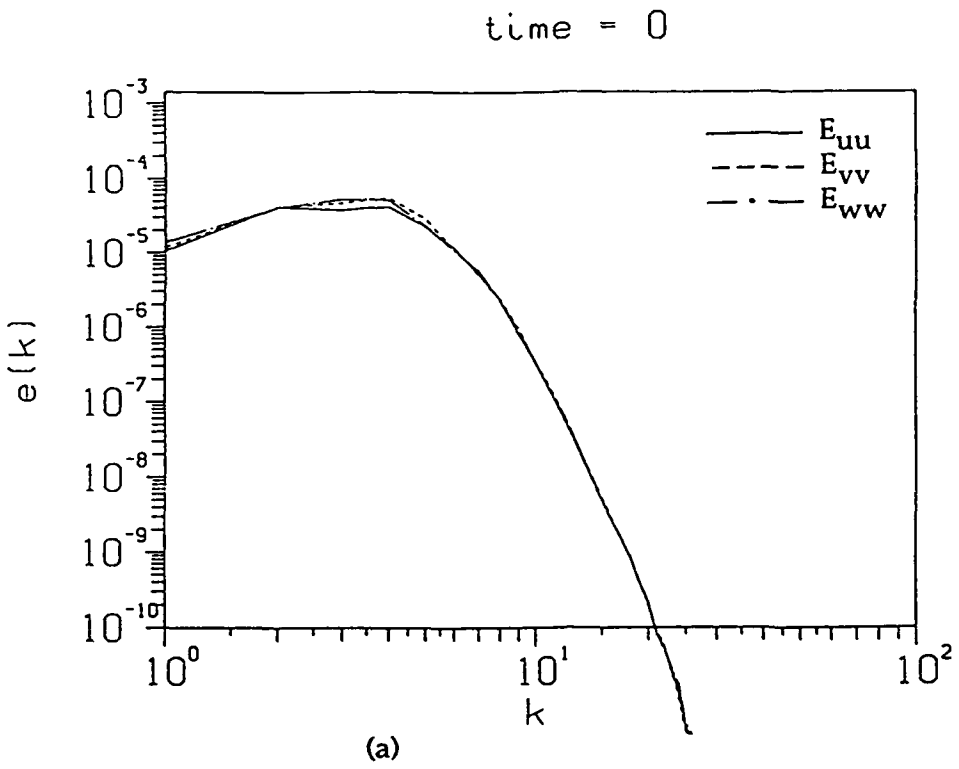

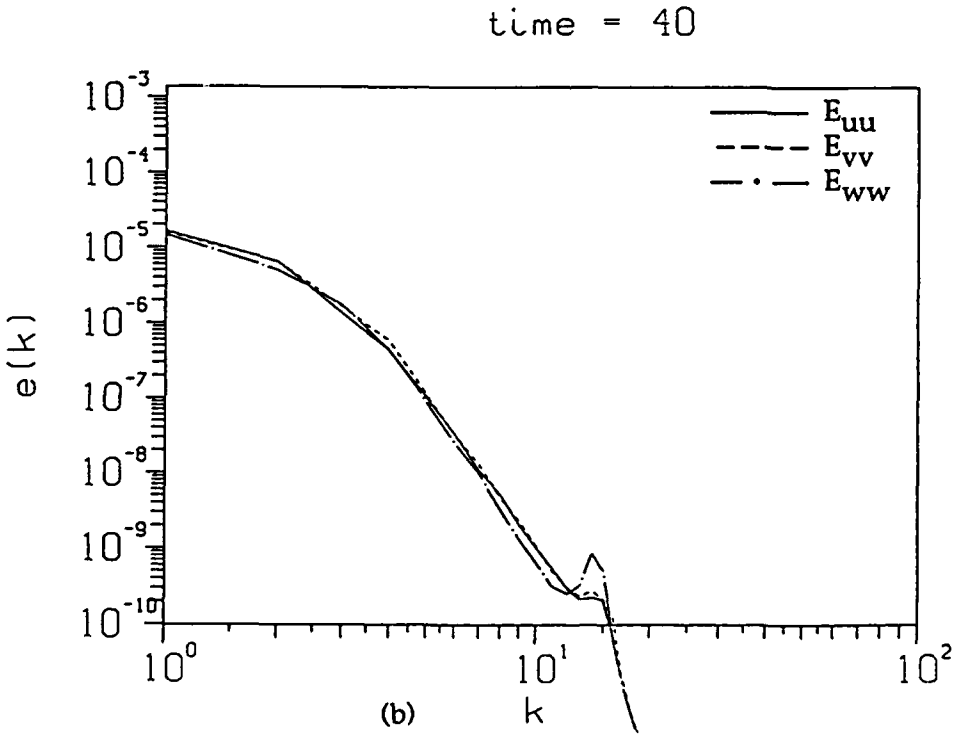

Figure 5.- Three-dimensional energy spectra of the horizontal and vertical velocity components, N=0.915, g=0.09, B-V period=69. (a) time = 0, (b) time = 40, (c) time = 80.

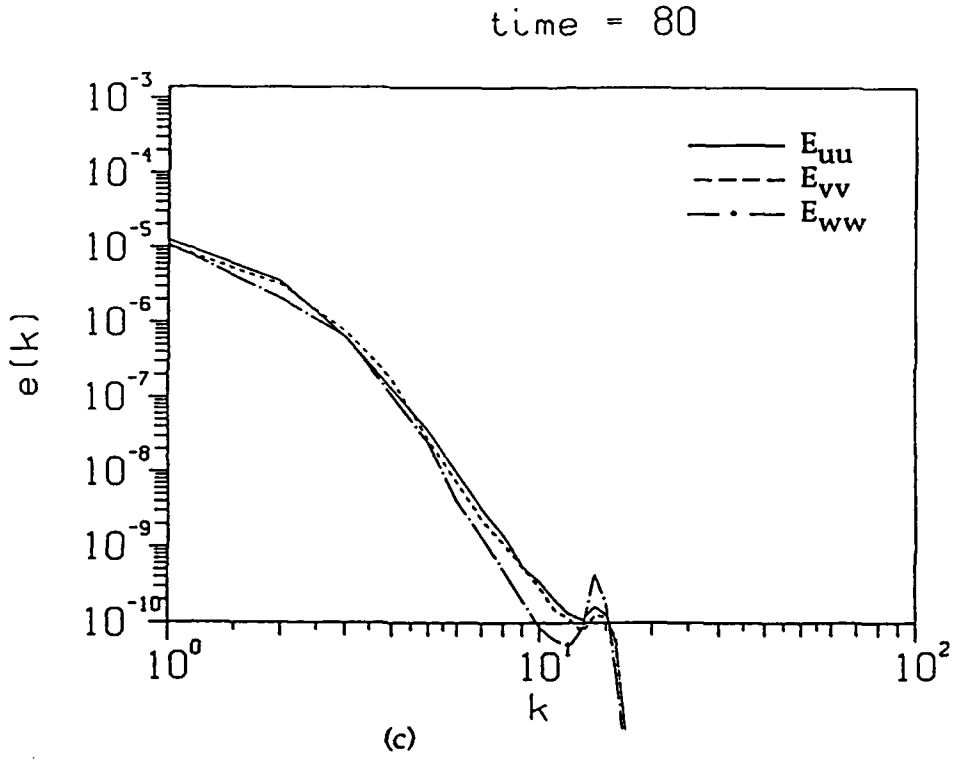

(c)

Figure 5.- continued.

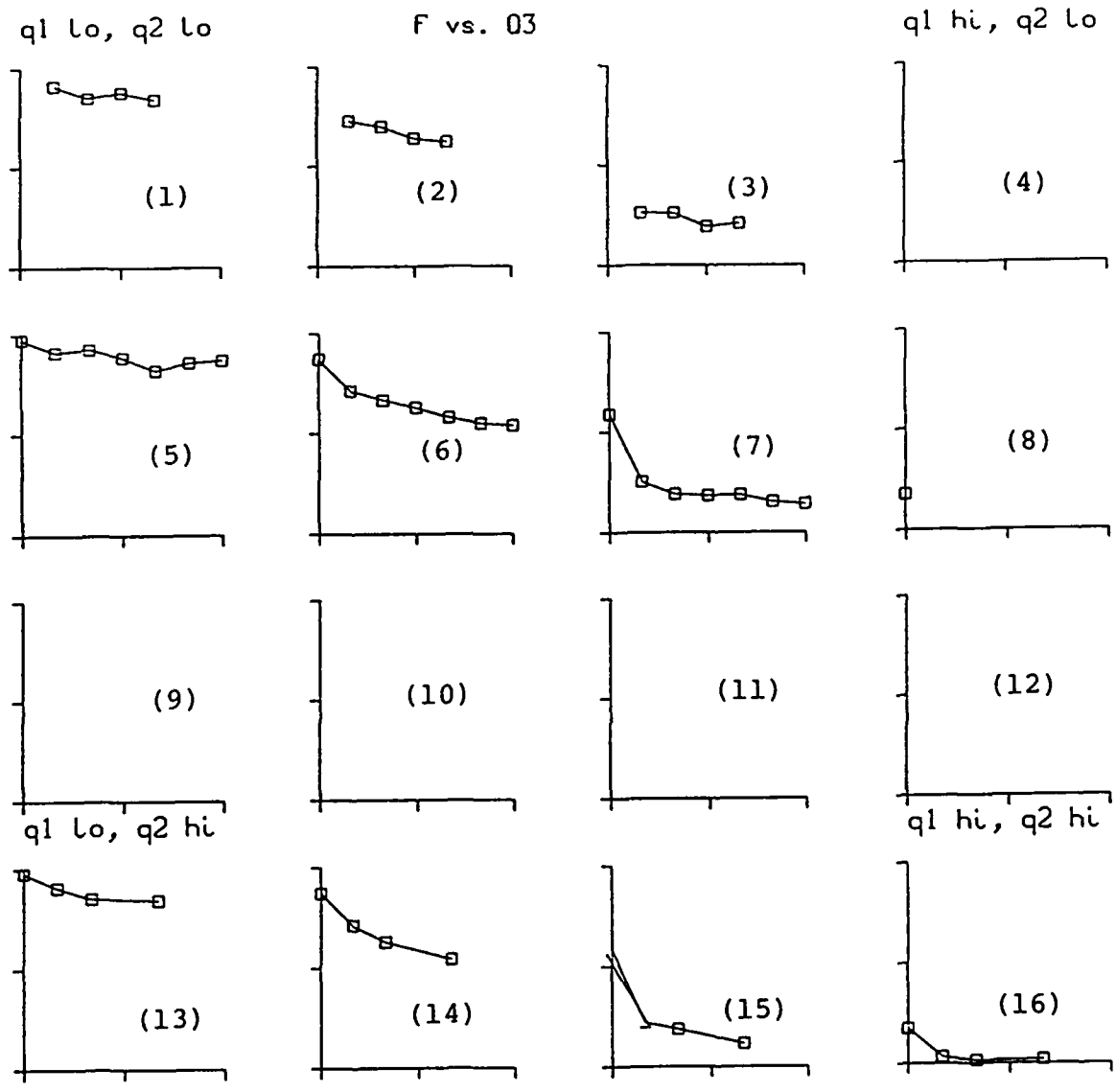

Figure 6.- Log-log plot of the density energy spectrum ($F = E_{\rho\rho}$) vs. time (Q3). Each subplot is for a different range of wavenumber (Q1) and B-V frequency (Q2). The regions are numbered from 1 to 16. Empty subplots mean that no data exists within those ranges.

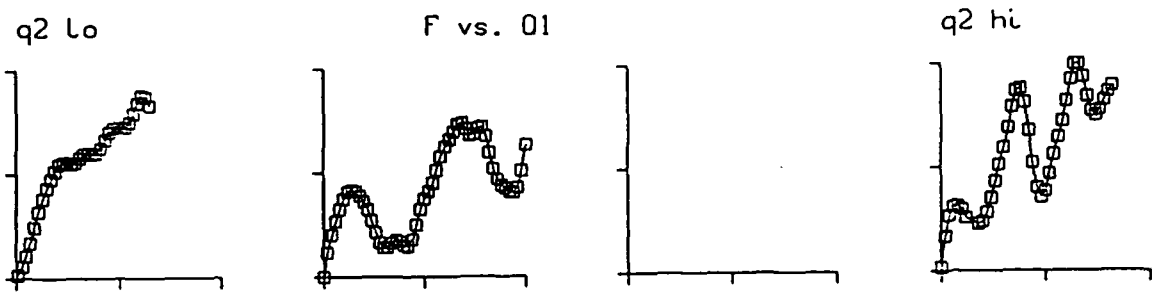

(a)

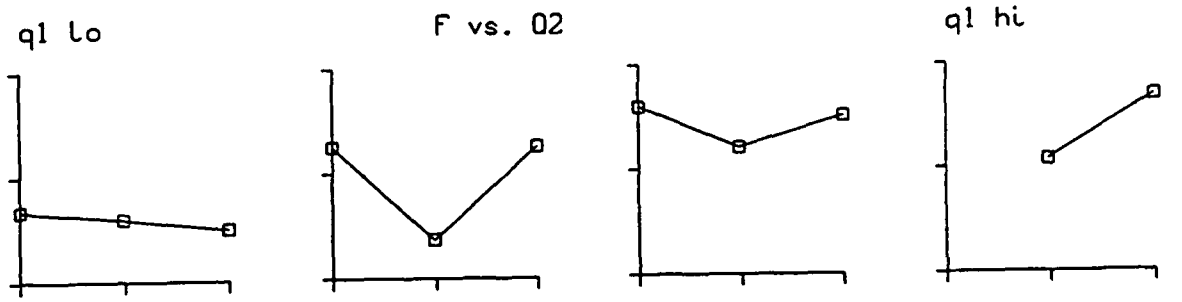

(b)

Figure 7.- (a) Vertical Taylor microscale (F) vs. time (Q1) for various B-V frequencies (Q2). (b) Vertical Taylor microscale (F) vs. B-V frequency (Q2) for various times (Q1).

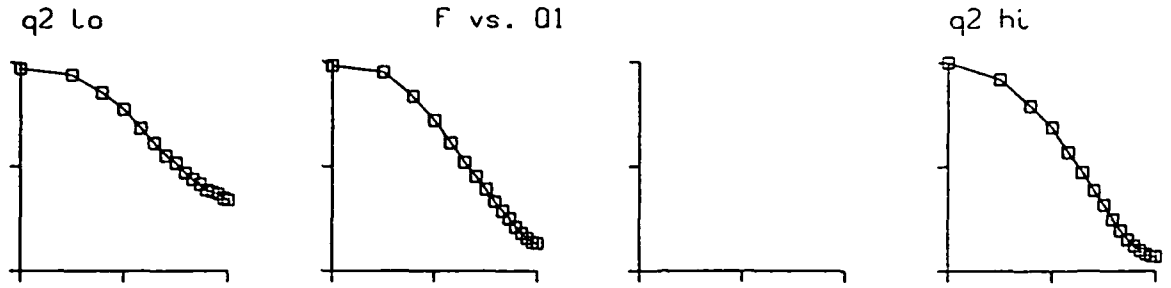

(a)

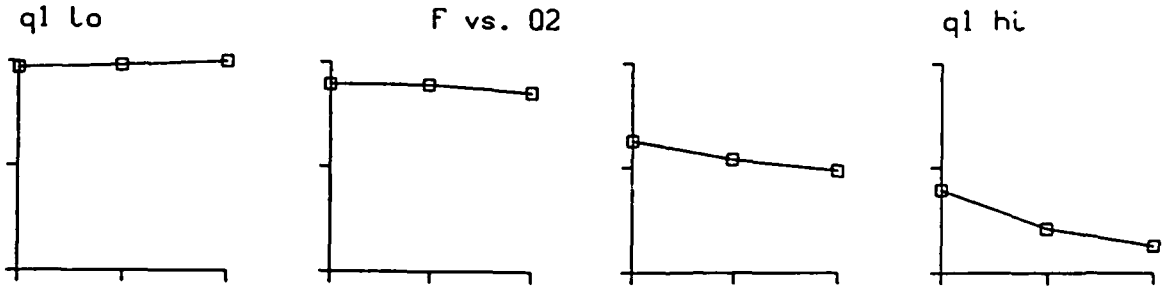

(b)

Figure 8.- (a) One-dimensional horizontal velocity energy spectrum (F) vs. wavenumber (Q1) for various B-V frequencies (Q2). (b) One-dimensional horizontal velocity energy spectrum (F) vs. B-V frequency (Q2) for various wavenumbers (Q1).

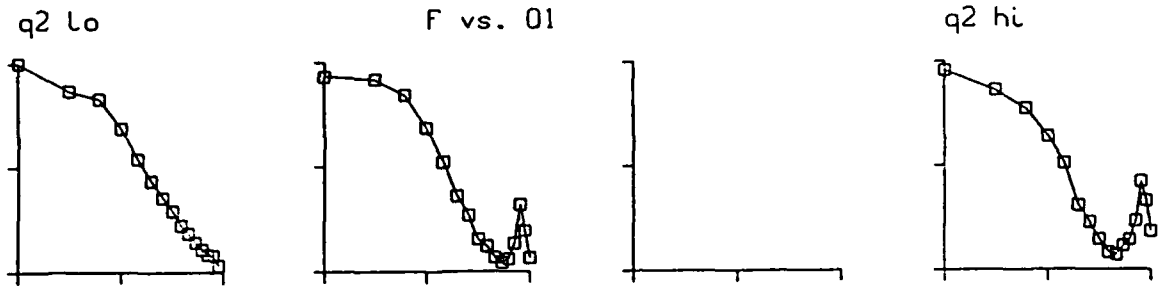

(a)

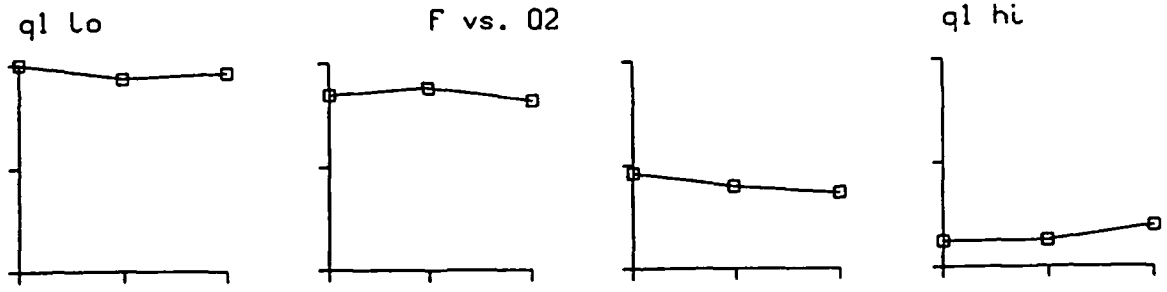

(b)

Figure 9.- (a) One-dimensional vertical velocity energy spectrum (F) vs. wavenumber (Q1) for various B-V frequencies (Q2). (b) One-dimensional vertical velocity energy spectrum (F) vs. B-V frequency (Q2) for various wavenumbers (Q1).

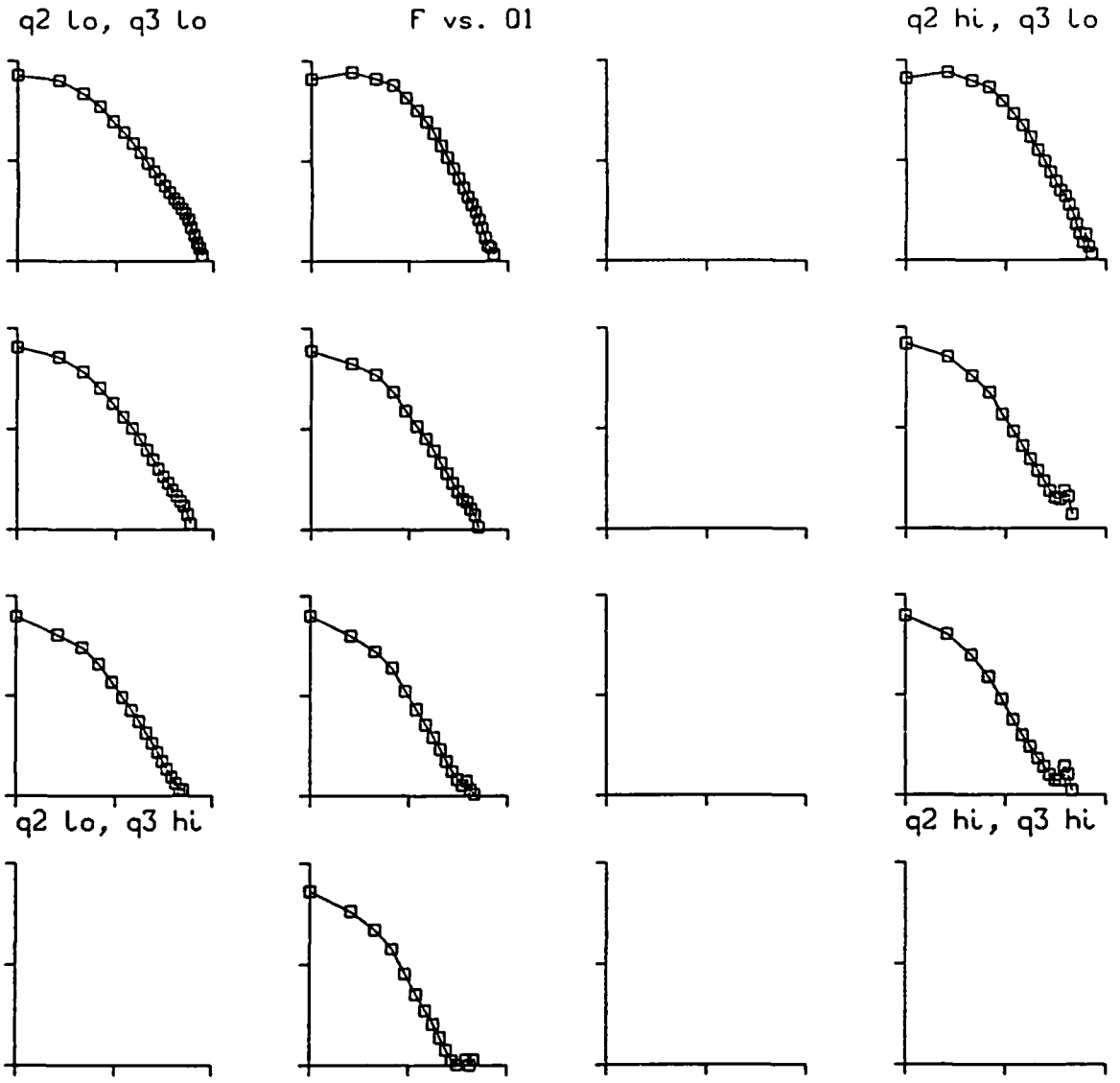

Figure 10a.- Log-log plot of the sum of spectral energies for each velocity component (F = $E_{ke} = E_{uu}+E_{vv}+E_{ww}$) vs. wavenumber (Q1). Each subplot is for a different range of B-V frequency (Q2) and time (Q3).

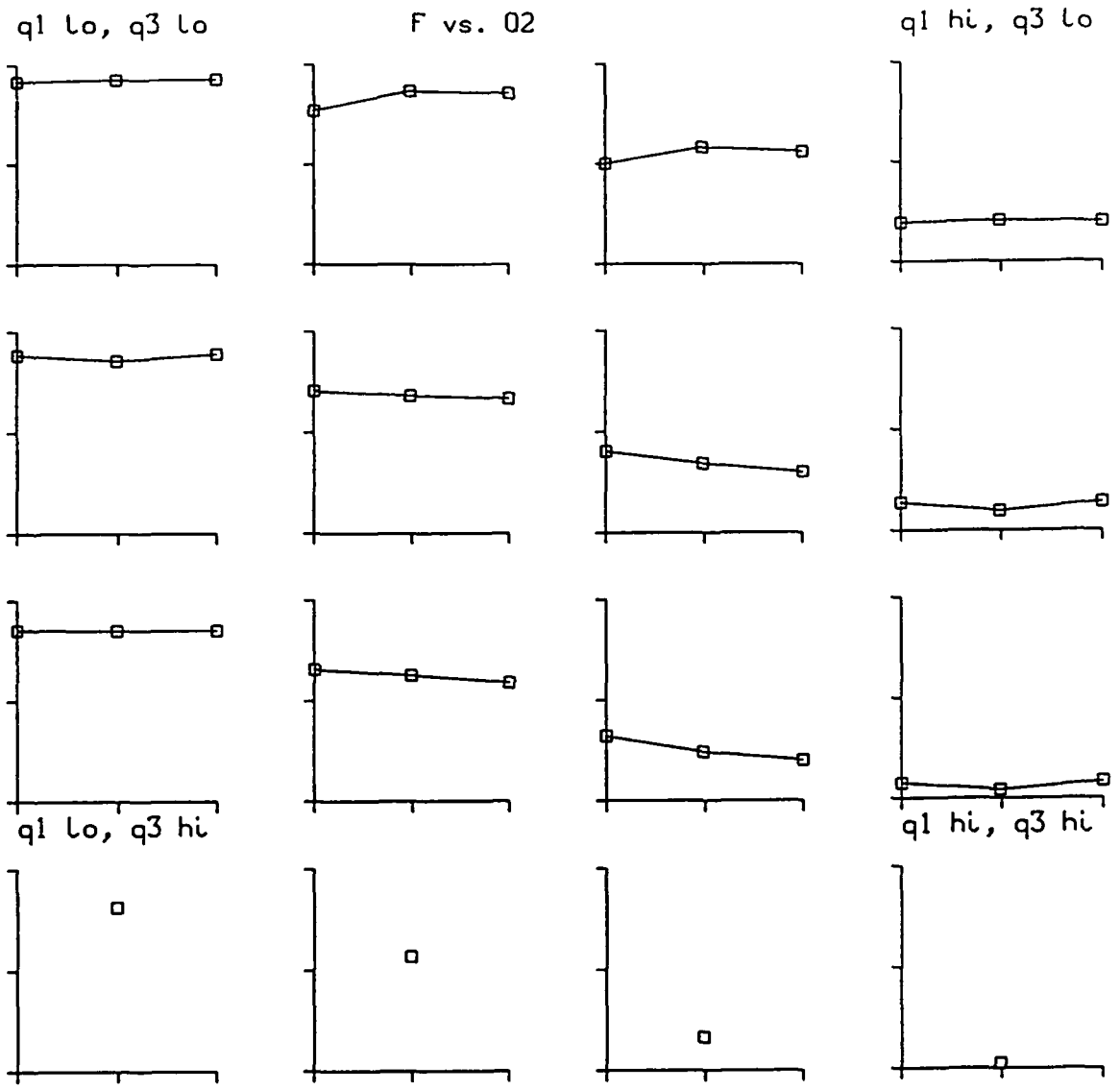

Figure 10b.- Log-log plot of the sum of spectral energies for each velocity component (F = $E_{ke} = E_{uu}+E_{vv}+E_{ww}$) vs. B-V frequency (Q2). Each subplot is for a different range of wavenumber (Q1) and time (Q3).

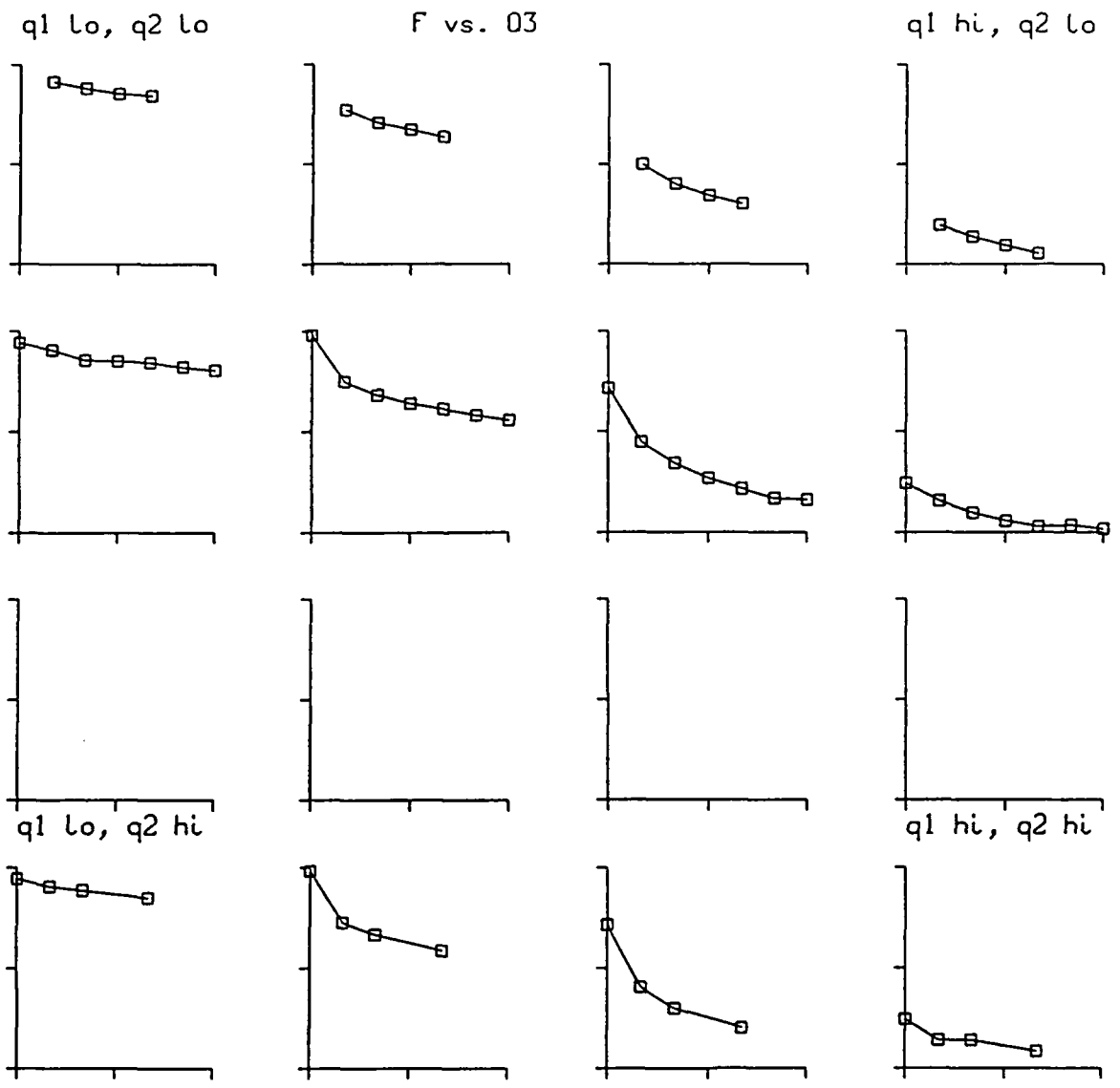

Figure 10c.- Log-log plot of the sum of spectral energies for each velocity component (F = $E_{ke} = E_{uu}+E_{vv}+E_{ww}$) vs. time (Q3). Each subplot is for a different range of wavenumber (Q1) and B-V frequency (Q2).

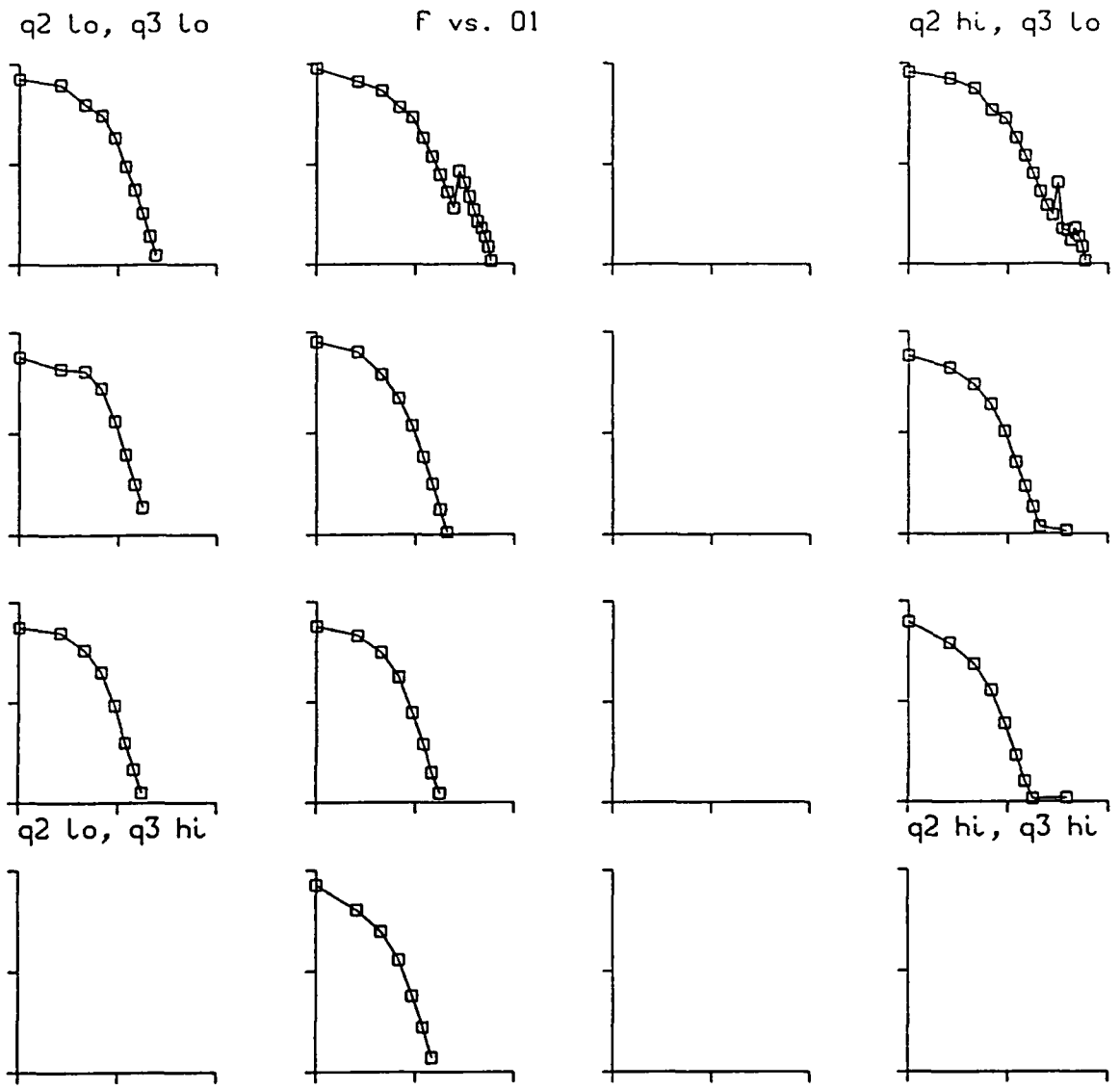

Figure 11a.- Log-log plot of the density energy spectrum ($F = E_{\rho\rho}$) vs. wavenumber (Q1). Each subplot is for a different range of B-V frequency (Q2) and time (Q3).

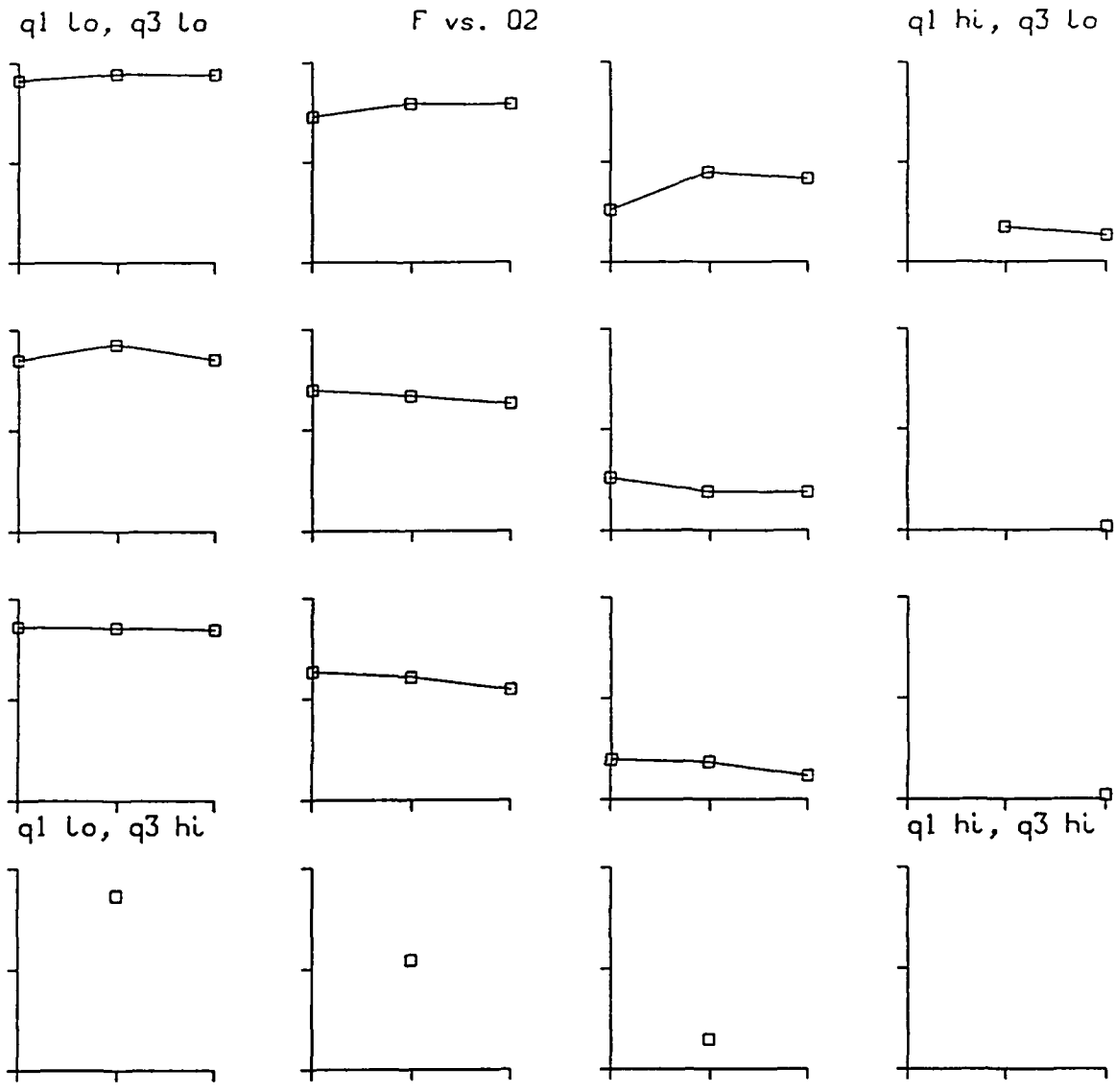

Figure 11b.- Log-log plot of the density energy spectrum ($F = E_{\rho\rho}$) vs. B-V frequency (Q2). Each subplot is for a different range of wavenumber (Q1) and time (Q3).

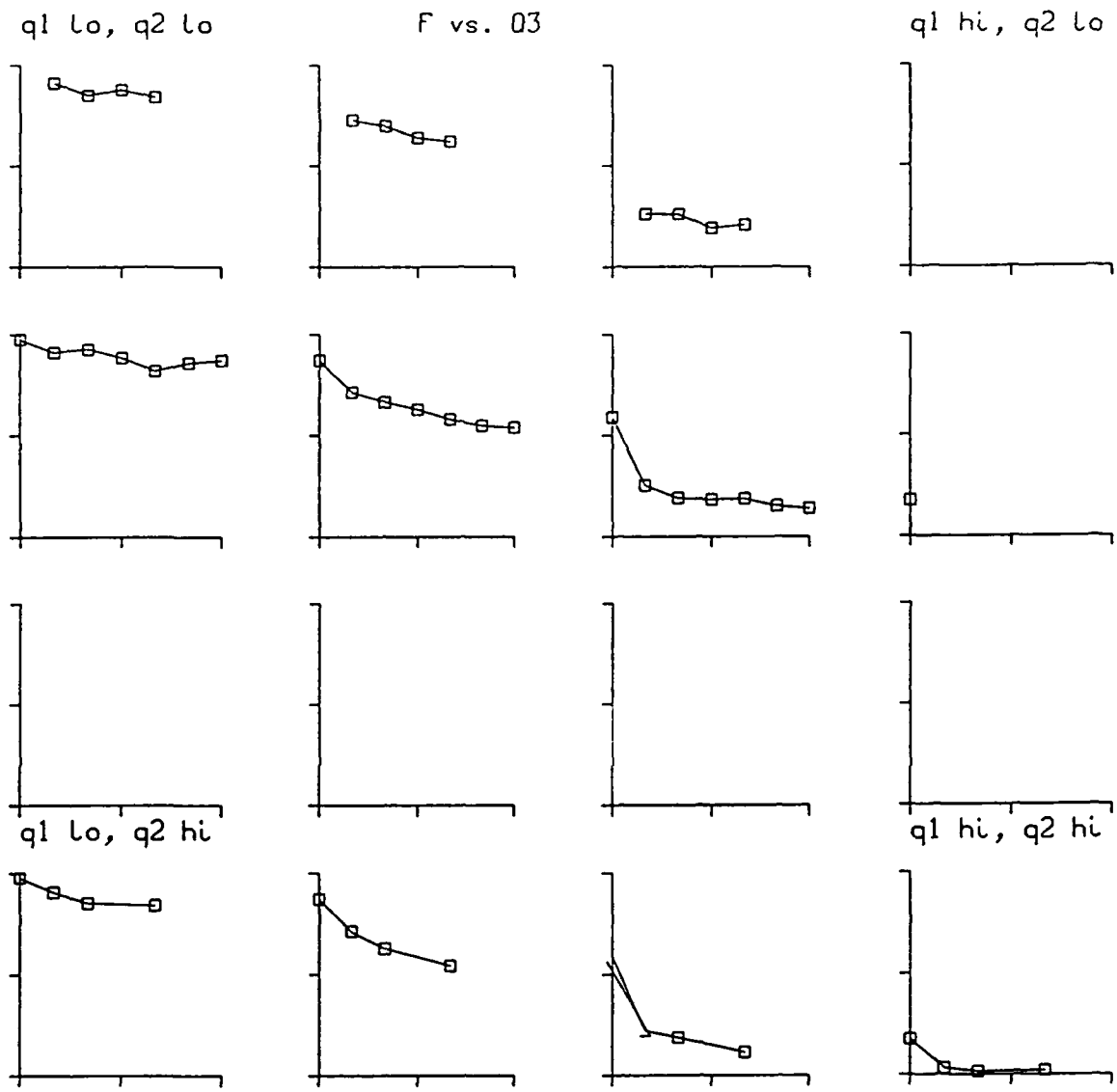

Figure 11c.- Log-log plot of the density energy spectrum ($F = E_{\rho\rho}$) vs. time (Q3). Each subplot is for a different range of wavenumber (Q1) and B-V frequency (Q2).

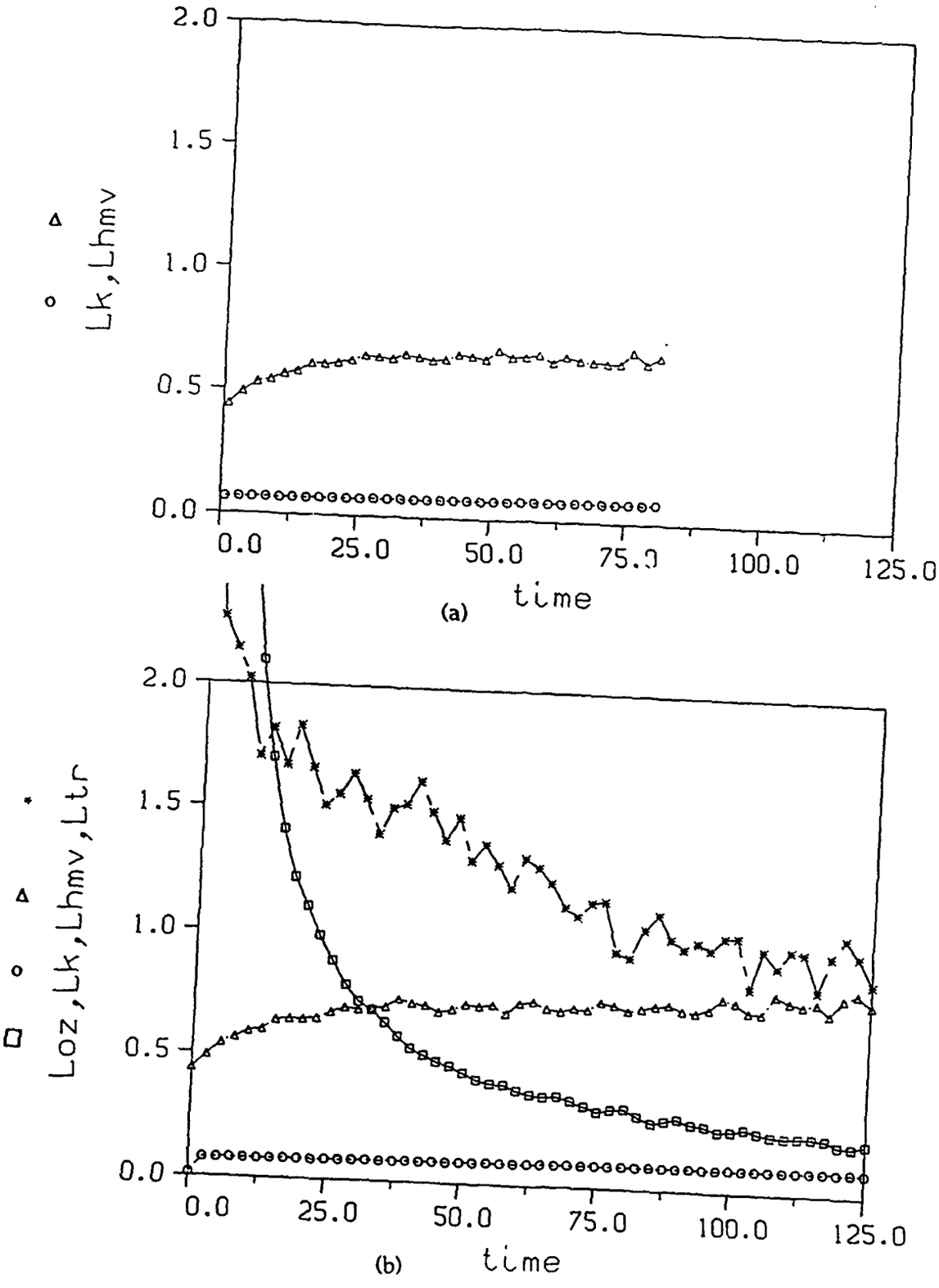

Figure 12.- Ozmidov (Loz), Kolmogorov (Lk), horizontal Taylor (Lhmv), and density turbulent (Ltr) length scales vs. time. (a) Unstratified, (b) Stratified (N=0.045, g=0.09, B-V period=140), (c) Stratified (N=0.0915, g=0.09, B-V period=69).

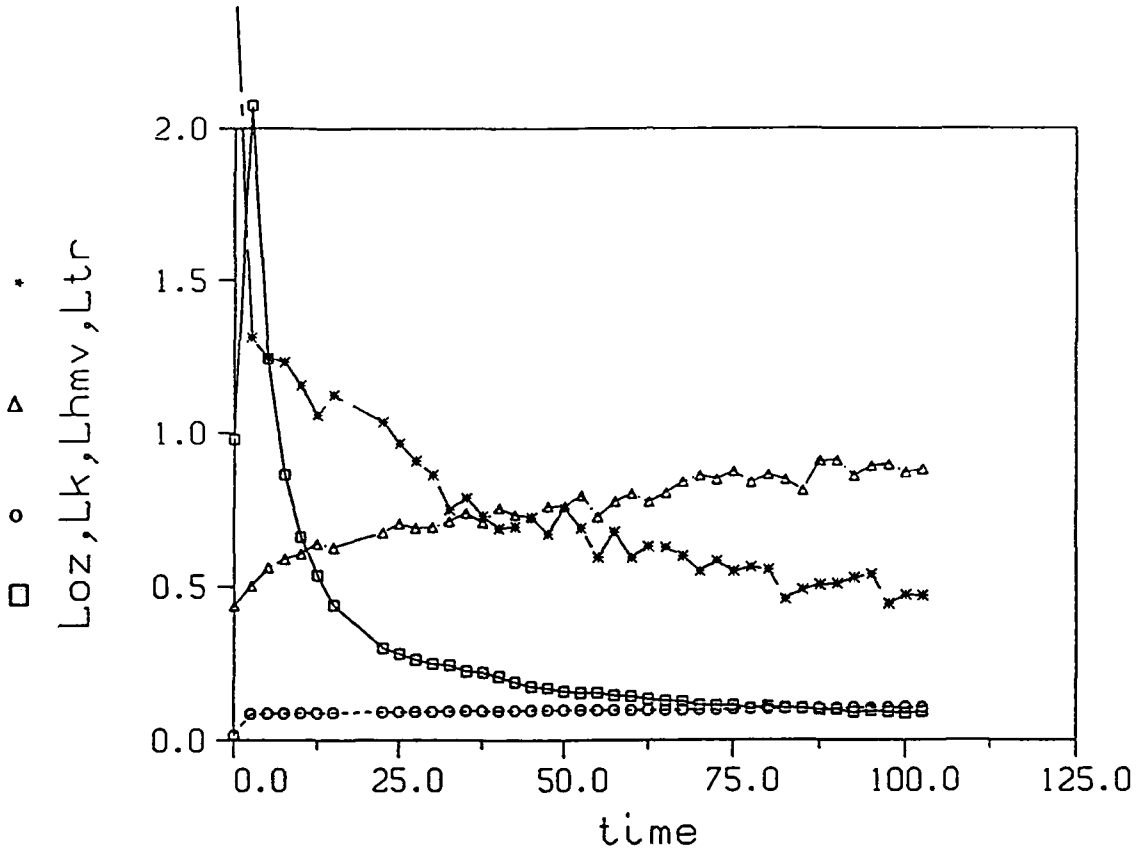

(c)

Figure 12.- continued.

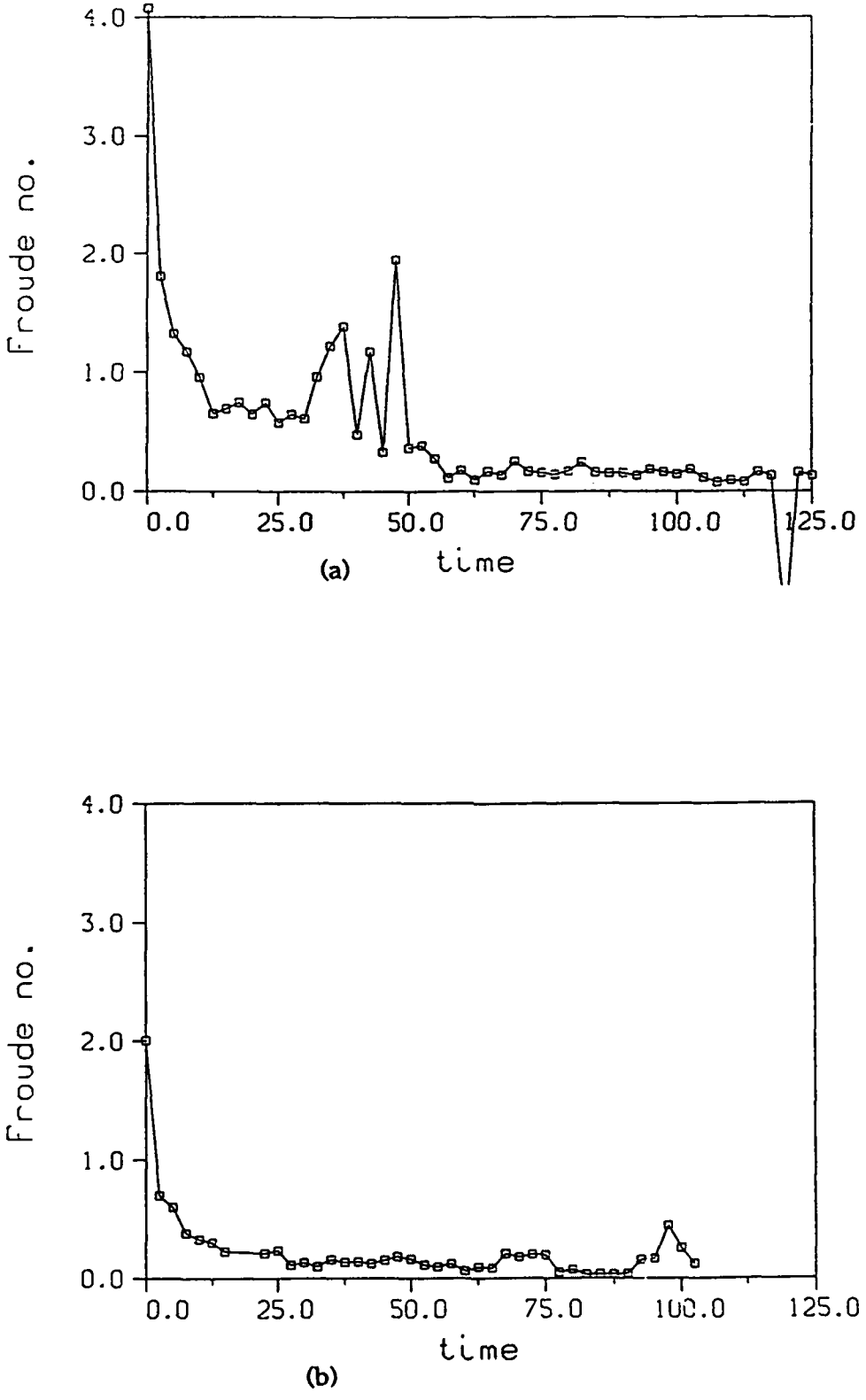

Figure 13.- Microscale Froude number vs. time. (a) Stratified (N=0.045, g=0.045, B-V period=140), (b) Stratified (N=0.0915, g=0.09, B-V period=69).

Appendix A

Derivation of Stratified Density and Pressure Gradients

Starting with the definition of the Brunt-Vaisala frequency, the equation of state for compressible flows, and the vertical momentum equation:

$$N^2 = \frac{g}{T}\left[\frac{\partial T}{\partial z} + \frac{g}{c_p}\right] \tag{A1}$$

where N = Brunt-Vaisala frequency
T = temperature
g = gravitational constant
c_p = specific heat at constant pressure = $\frac{\gamma}{\gamma-1}$ = 3.5 for air since gas constant R = 1
and γ = ratio of specific heats = 1.4

$$p(z) = \rho(z)T(z) \tag{A2}$$

where ρ = density
p = pressure

$$\frac{\partial p}{\partial z} = -\rho g \quad \text{(no mean flow)} \tag{A3}$$

The differential equation for the temperature can be solved, giving

$$T(z) = \frac{g^2}{c_p N^2} + c\exp\left[\frac{N^2}{g}z\right]$$

and choosing the boundary condition $T = \frac{1}{\gamma}$ at z = 0, gives the constant of integration $c = \frac{1}{\gamma} - \frac{g^2}{c_p N^2}$

Thus the temperature distribution in stratified flow is

$$T(z) = \frac{g^2}{c_p N^2} + \left[\frac{1}{\gamma} - \frac{g^2}{c_p N^2}\right]\exp\left[\frac{N^2}{g}z\right] \tag{A4}$$

(A2), (A3), and (A4) can be solved together to get the pressure and density distributions as functions of z, N, and g.

$$\frac{\partial p}{\partial z} = \rho \frac{\partial T}{\partial z} + T \frac{\partial \rho}{\partial z} \tag{A5}$$

$$-\rho g = \rho \frac{\partial T}{\partial z} + T \frac{\partial \rho}{\partial z} \tag{A6}$$

$$\frac{\partial \rho}{\partial z} + \left[\frac{1}{T} \frac{\partial T}{\partial z} + \frac{g}{T} \right] \rho = 0 \tag{A7}$$

$$\frac{\partial T}{\partial z} = \left[\frac{1}{\gamma} - \frac{g^2}{c_p N^2} \right] \left[\frac{N^2}{g} \right] \exp \left[\frac{N^2}{g} z \right] \tag{A8}$$

(A4) and (A8) combined with (A7) give a differential equation for the density which can be solved to give

$$\rho(z) = c \left[\exp(-mz) \exp\left[-\frac{g}{b} z \right] \left[e + b \exp(-mz) \right]^{-1} \left[b + e \exp(mz) \right]^{c_p} \right] \tag{A9}$$

where $b = \dfrac{g^2}{c_p N^2}$, $e = \left[\dfrac{1}{\gamma} - b \right]$, $m = \dfrac{N^2}{g}$

and the constant of integration $c = \left[\dfrac{1}{\gamma} \right]^{1-c_p}$

using the boundary condition $\rho = 1.0$ at $z = 0$.

The pressure distribution p(z) is found from (A2), (A4), and (A9).

The boundary condition for the pressure is $p(0) = \dfrac{1}{\gamma}$.

These equations were solved for different values of N and g, and the results are plotted in Figure 1 of the main report.